

Substellar Mass Function of Young Open Clusters as Determined through a Statistical Approach Using 2MASS and GSC Data

Anandmayee Tej^{1,2,3}, Kailash C. Sahu¹, T. Chandrasekhar² & N.M. Ashok²
 E-mail: tej@newb6.u-strasbg.fr, ksahu@stsci.edu, chandra@prl.ernet.in, ashok@prl.ernet.in

ABSTRACT

In this paper we present the mass functions in the substellar regime of three young open clusters, IC 348, σ Orionis and Pleiades, as derived using the data from the 2 Micron All Sky Survey (2MASS) catalogue which has a limiting magnitude of $K_s \sim 15$, and the latest version of the Guide Star Catalogue (GSC) which has a limiting magnitude of $F^4 \sim 21$. Based on recent evolutionary models for low mass stars, we have formulated the selection criteria for stars with masses below $0.5M_\odot$. Using a statistical approach to correct for the background contamination, we derive the mass function of objects with masses ranging from $0.5M_\odot$ down to the substellar domain, well below the Hydrogen Burning Mass Limit. The lowest mass bins in our analysis are 0.025, 0.045 and 0.055 M_\odot for IC 348, σ Orionis and Pleiades, respectively. The resultant slopes of the mass functions are 0.8 ± 0.2 for IC 348, 1.2 ± 0.2 for σ Orionis and 0.5 ± 0.2 for Pleiades, which are consistent with the previous results. The contribution of objects below $0.5 M_\odot$ to the total mass of the cluster is $\sim 40\%$, and the contribution of objects below $0.08 M_\odot$ to the total mass is $\sim 4\%$.

1. Introduction

The Initial Mass Function (IMF) of stars is one of the most fundamental and crucial ingredients in models of galaxy formation and stellar evolution. It determines several key parameters in stellar populations, such as the yield of heavy elements, the mass-to-light ratio, luminosity evolution over time, and the energy input into the interstellar medium. The determination of the IMF is therefore of great astrophysical importance. The IMF of low-mass stars is of special interest in this context, since they contain a major fraction of the stellar mass, and have been hypothesized to contain a

¹Space Telescope Science Institute, 3700 San Martin Drive, Baltimore, MD 21218, USA

²Physical Research Laboratory, Navrangpura, Ahmedabad - 380009, India

³Present Affiliation: Observatoire Astronomique de Strasbourg, 67000 Strasbourg, France

⁴F refers to the POSS II IIIa-F passband

significant fraction of the total mass in the Universe (see, e.g., Fukugita, Hogan and Peebles, 1998). In this paper we mainly deal with objects having masses less than $0.5M_{\odot}$, the lowest mass of the detectable objects being as low as $0.025M_{\odot}$. These low-mass stars evolve little over the lifetime of the Universe, and hence the observed present day Mass Function of these stars is likely to be a good representation of their IMF. But, the IMF at or below the HBML remains poorly known, mainly for two reasons. First, such objects are faint and hence difficult to detect. Second, the mass-luminosity relation of these objects is uncertain and model-dependent, and hence their mass determination is imprecise. Significant improvements are being made on both these aspects, as described below.

The difficulty caused by their faintness can be greatly alleviated by concentrating on young, low-mass objects since the low-mass stars at or below the HBML are expected to be warmer and more luminous when young, although they rapidly cool and fade with age (Burrows et al. 1997, D’Antona & Mazzitelli 1997, Baraffe et al. 1998). Hence young and nearby open clusters provide a good opportunity to study the low end of the stellar IMF, since the suitable combination of their youth and proximity makes it possible to detect objects well below the HBML in these clusters, particularly at near-infrared wavelengths.

The uncertainty in the mass-luminosity relation has been greatly reduced by the tremendous progress in the theoretical models for the evolution of these cool and dense objects over the past few years. These models play a crucial role in predicting masses of these low-mass objects from the observable quantities like colors and luminosities. Burrows et al. (1997) have generated models of spectra, colors and evolution of brown dwarfs using nongrey calculations. Their models span the mass range of $0.3M_J$ to $70M_J$ (where M_J refers to the mass of Jupiter) with effective temperatures varying from ~ 1300 K to 100 K. D’Antona & Mazzitelli (1997) simulate the evolution of objects in the mass range $20M_J \leq M \leq 1.5M_{\odot}$. They describe the star’s evolution from the hydrostatic phases of pre-main sequence contraction to the hydrogen burning main sequence phase through deuterium and lithium burning. Baraffe et al.(1998) have developed the evolutionary models in the $0.075 M_{\odot}$ to $1 M_{\odot}$ mass range for solar type metallicities based on the NextGen atmospheric models of Allard et al. (1996), and Chabrier et al. (2000) have extended this study by including dust formation and opacity. The recent models for dwarfs by Marley et al (2002) take the extra effect of sedimentation into account, which suggest that some of the colors, particularly the Sloan $i'-z'$, can be greatly affected by sedimentation.

The advent of the red-sensitive CCDs and 2-dimensional near-IR detectors in the last decade has made it possible to detect such low-mass objects, and there have been numerous imaging surveys targeted towards open clusters to probe the substellar domain. Surveys by Wilking et al. (1999) and Luhman et al. (1999) for ρ Ophiuchi, Herbig (1998) and Luhman (1999) for IC 348, Béjar et al. (1999) and Zapatero Osorio et al. (1999a) for σ Orionis, Zapatero Osorio et al. (1996) and Stauffer et al. (1999) for α Persei, Zapatero Osorio et al. (1997;1999b), Bouvier et al. (1998) and Hambly et al. (1999) for Pleiades, Hambly et al. (1995), Pinfield et al. (1997) and Magazzù et al.(1998) for Praesepe, Gizis et al. (1999) and Reid & Hawley (1999) for Hyades, and Barrado y

Navascués et al. (2001a) for IC 2391 are to name a few.

The recent release of the 2MASS catalogue in the near-infrared wavelengths with a limiting magnitude of $K_s \sim 15$, and the latest (development) version of the Guide Star Catalogue (GSC) with a limiting magnitude of $F \sim 21$ form an ideal combination to study low-mass objects in nearby open clusters using a statistical approach. We have used these two datasets in conjunction with the recent evolutionary models to isolate the low mass members of the clusters. The cluster membership is not ascertained by follow-up spectroscopy or proper motion studies. But the background/foreground contamination is accounted for statistically by studying nearby control fields. In §2, we review some previous work on the derivation of the mass function; in §3, we describe the rationale of our sample selection and the details of the 3 individual clusters selected for this study; in §4, we describe the data, the procedure adapted in selecting the cluster members and the method used for their mass determination; in §5, we describe the specific selection criteria used for the individual clusters and the slope of the resultant mass function; and we end with a discussion of the results in §6. We plan to extend this work to more clusters in the future.

2. The Mass Function

The stellar mass function is defined as the number density of stars per unit mass bin, and is universally represented as

$$\Psi(M) = \frac{dN}{dM} \quad \text{stars } pc^{-3} M_{\odot}^{-1} \quad (1)$$

The stellar IMF for the high-mass stars ($M > 1M_{\odot}$) has been long established and well studied following the pioneering work of Salpeter (1955). Salpeter (1955) derived the IMF from the luminosity function of the present day field stars assuming a constant rate of star formation and correcting for the stellar evolution. In linear units the Salpeter mass function is given by

$$\Psi(M) \propto M^{-\alpha} \quad \text{stars } pc^{-3} M_{\odot}^{-1} \quad (2)$$

where $\alpha = 2.35$ for stars in the mass range $1-10 M_{\odot}$. The steep slope of the IMF indicates that the low-mass stars greatly outnumber their high-mass counterparts and account for the major fraction of the stellar mass. Miller & Scalo (1979) and Scalo (1986) rederived the stellar IMF by extending the study to the subsolar domain. Their derived values of α are 1.4, 2.5 and 3.3 for the mass ranges $0.1M_{\odot} \leq M \leq 1.0M_{\odot}$, $1.0M_{\odot} \leq M \leq 10M_{\odot}$ and $10M_{\odot} \leq M$, respectively.

There have been several studies recently to extend the stellar mass function to lower masses. Kroupa et al (1993) took the age and metallicity dependence of the mass-luminosity relation into account in determining the mass functions. Their derived values of α are 2.7 for stars more massive than $1 M_{\odot}$, 2.2 in the mass range $0.5-1M_{\odot}$ and $0.7 < \alpha < 1.85$ in the range $0.08-0.5M_{\odot}$. Chabrier

(2001) has derived the stellar mass function of the Galactic disk stars down to the vicinity of the HBML using their luminosities determined from parallax measurements. His study indicates that the mass function may be slightly better represented by a log-normal or exponential form than the power-law form given by Eq. 1. His results suggest that the mass function flattens out below $1 M_{\odot}$ but keeps rising down to the bottom of the main sequence which is consistent with the results of Kroupa et al (1993).

All these studies suggest a flattening of the IMF at the low mass end. However, the nature of the mass function below the HBML, and particularly its spatial variation if any, is still poorly known. On the other hand, to understand the Galactic structure, it is important to know the temporal and spatial variation of the IMF.

According to the study by Adams & Fatuzzo (1996), the IMF shows a low mass turn over and they attribute this turn over to the suppression of the very formation of low-mass objects by winds. Models by Price & Podsiadlowski (1995) suggest that the stellar IMF of a cluster should depend on the cluster density because of the stellar interactions during the process of accretion. Whereas, Larson (1992) links the dependence of the stellar IMF on the geometrical structure of star forming clouds and in particular, he attributes the power law form of the upper IMF to the presence of hierarchical or fractal structure in these clouds. The fragmentation of these filaments is predicted to yield a minimum stellar mass of $\sim 0.1 M_{\odot}$.

The searches for low-mass objects in young clusters by various groups mentioned in §1 have also found many hundreds of candidates with estimated masses below the hydrogen-burning limit of $\sim 0.075 M_{\odot}$. In addition, some of these searches have also discovered free-floating objects with inferred masses possibly below the deuterium-burning limit of $\sim 0.013 M_{\odot}$ (see, e.g. Lucas & Roche 2000; Zapatero Osorio et al. 2000). The scenarios proposed for the formation of such low-mass objects generally involve ejections from a multiple system. Reipurth & Clarke (2001) argue that brown dwarfs are not formed as a result of low mass core collapse but they are ejected stellar embryos from multiple systems for which the star formation process was aborted before the onset of hydrogen burning. This ejection model could appreciably explain the flattening of the IMF at low masses. Boss (2001) has suggested that, under certain conditions, the same collapse and fragmentation process that produce single and multiple stars can also produce planetary-mass, self-gravitating objects. The ejection of these fragments from an unstable, protostellar system may explain the formation of the free-floating planetary-mass objects found in some young clusters.

Reid et al. (1999) derive the mass function of the field stars using the 2MASS and the DENIS data within 8 pc of the Sun in the mass range $0.1 - 1 M_{\odot}$. Their study shows that in the lower mass range the mass function is flatter ($1 \leq \alpha \leq 2$), the value of α being closer to the lower limit. Extrapolating their results to the substellar regime down to $0.01 M_{\odot}$ they predict that the ratio of the number of brown dwarfs to the main sequence stars is 2:1 in the solar neighborhood. Their study implies that brown dwarfs contribute less than 15% of the total mass of the disk and hence they are unlikely to be the major constituent of Galactic dark matter. However, their mass

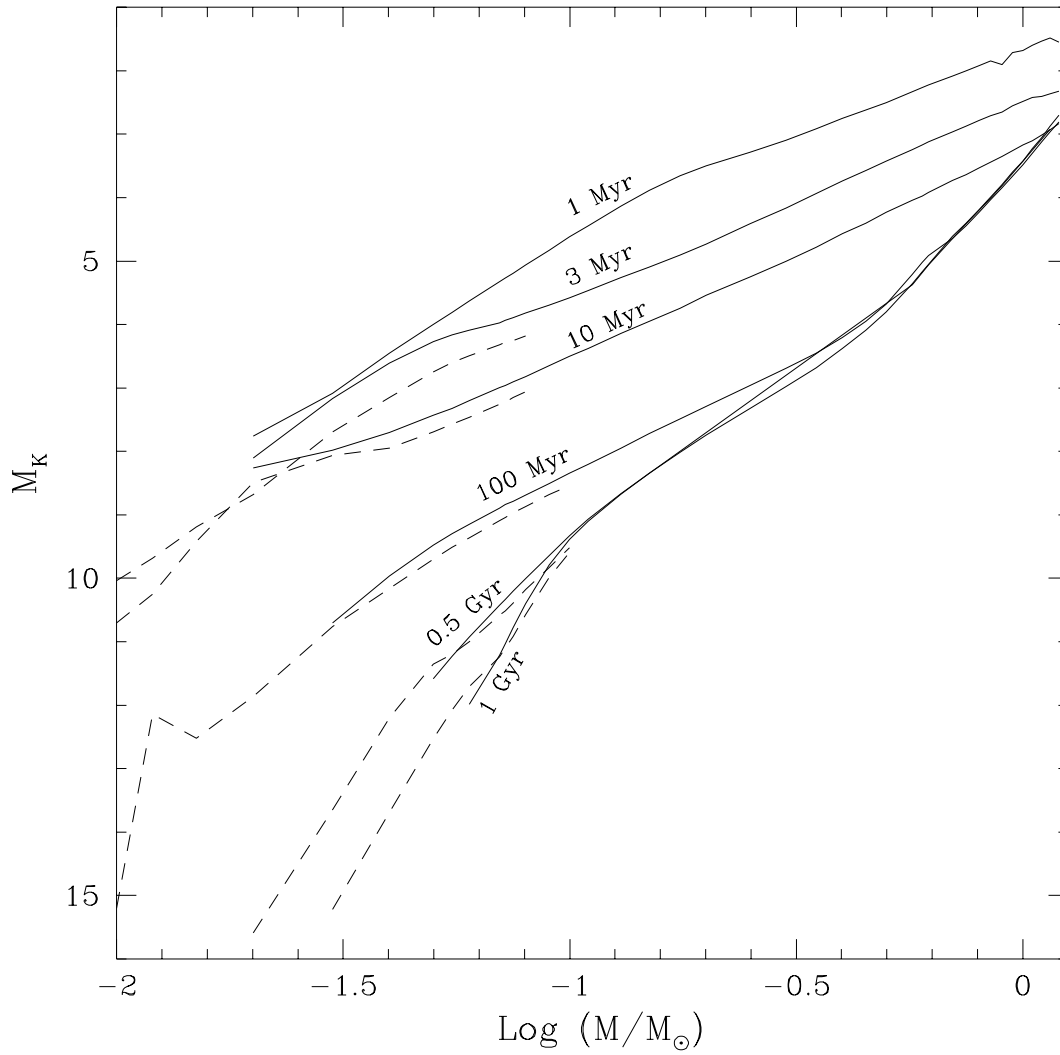


Fig. 1.— In this figure we show the absolute K magnitudes as a function of mass (in logarithmic units) for different ages. The isochrones are from the models by Baraffe et al. (1998) (solid lines) and the Dusty models by Chabrier et al. (2000) (dashed lines).

function is necessarily derived from a mixed sample of stars formed at different times and different environments.

Studying the stellar IMF in different clusters provides a means to check whether the IMF in clusters is different from that of the field population and also to check the universality of the IMF. Low mass objects can, in principle, escape a cluster due to cluster dynamics and Galactic tides. In addition, the internal velocity dispersion may result in mass segregation in the cluster which is expected to increase with cluster age (Spitzer & Mathieu 1980; Kroupa 1995). However, clusters younger than one relaxation time should not show these effects. Mass segregation has been observed in very young (≤ 1 Myr) clusters such as the Orion Trapezium (Hillenbrand & Hartman 1997), but these are most likely the result of the formation process rather than the dynamical evolution. The typical relaxation time of clusters like Pleiades is ~ 10 Myr (Raboud & Mermilliod 1998). Hence, clusters with ages younger than ~ 10 Myr would be ideal to understand the mass function at the low mass regime, as these clusters are not old enough to have lost members due to stellar evolution, or to have suffered mass segregation due to dynamical effects such as evaporation or violent relaxation (Lada & Lada 1991 and references therein). Moreover, young clusters are ideally suited for the detection of very low mass objects and brown dwarfs and hence for deriving the mass function in the substellar domain. This fact can be better appreciated in Figure 1 which shows the K magnitudes as a function of age and mass of the low-mass objects. The figure, which uses the models of Baraffe et al. (1998)¹ and Chabrier et al. (2000), shows that objects with masses less than $0.1 M_{\odot}$ are more than 5 magnitudes brighter when they are 1 Myr old than when they are 1 Gyr old, which makes them more easily detectable.

3. Sample Selection

The main objective of the present study is to derive the stellar mass function down to very low masses for a sample of young open clusters, in an attempt to obtain a global view of the mass function of low-mass objects in such young clusters. Low mass stars ($M \leq 0.5M_{\odot}$) have effective temperatures below 3500 K (Berriman & Reid 1987) and brown dwarfs ($M \leq 0.08M_{\odot}$) have temperatures below 2800 K (Chabrier et al. 2000), which implies that the spectral energy distribution of these objects peaks in the near infrared between $1 - 3 \mu\text{m}$. Hence, the near IR bands are ideal for detecting these objects. We use the data from the 2MASS Second Incremental Release and the latest version of the GSC catalogue. This 2MASS release covers $\sim 47\%$ of the sky in JHK_s near-IR bands. Fortunately, it covers the major area of the three clusters and their corresponding control fields chosen by us. The incomplete coverage of our fields by the 2MASS data is accounted for by appropriate normalization as explained in §5. The latest version of the GSC catalog is an

¹The model isochrones in the published version constitute a subset of the available models and go down to $0.075M_{\odot}$. A larger set of model isochrones spanning a more extensive grid of ages and masses are available electronically via anonymous ftp from *ftp.ens-lyon.fr*.

all-sky catalog of stars in the $IIIa - J$ and F bands with limiting magnitudes of 22 and 21 in each passband respectively. (Currently, this catalog has restricted access, and is in its final stages of preparations for release, expected to be in late 2002, McLean private communication²). The red plates used in making the GSC catalogue had used slightly different emulsions for the Northern and the Southern surveys. Accordingly, the F-passbands are slightly different for the northern and the southern sources, which we have taken into account in our analysis of the three clusters. The 2MASS catalogue³ has roll over limiting magnitudes of 15 in K_s , 15.5 in H and 16.5 in J (the photometric accuracies are shown in Fig. 7 of the documentation pages of the 2MASS Second Incremental Release). This allows us to probe low-mass objects down to about $0.03 M_{\odot}$ of all nearby clusters ($D < 200\text{pc}$) with ages less than about 100 Myr (see Fig. 2).

Unlike most other previous studies which rely on confirming the candidate low-mass objects through spectroscopic observations, we use a statistical approach to estimate the number of low-mass objects. In a statistical approach, it is important to use several control fields close to each cluster to subtract the contribution of foreground and background objects. The nature of these two extended surveys enables us to use several such control fields and we are not limited by our choice of the field sizes for the clusters or the control fields. To establish the viability of a statistical approach, it is important to apply this procedure for a few well-studied clusters. The clusters we have chosen for this work are Pleiades, IC 348 and σ Orionis, all of which are young and nearby. The masses of the objects corresponding to the faint limiting magnitudes in each passband for the 3 clusters are given in Table 1. For IC 348 and σ Orionis, a member with mass $\sim 0.025 M_{\odot}$ would have a K_s magnitude ~ 15 and for the relatively older cluster Pleiades, $K_S \sim 15$ corresponds to objects with masses $\sim 0.04 M_{\odot}$. Pleiades and IC 348 have been well-studied through ground-based optical and near-IR photometry and optical spectroscopy, and hence it would be useful to check the consistency of our results with that of the previous studies. Previous studies of σ Orionis are confined to photometry in optical wavelengths, but our study includes the near IR data. A brief description of the individual clusters is given below. The details of the derivation of mass functions and comparison with other studies will be discussed in a later section.

3.1. IC 348

IC 348 is a relatively dense, rich and compact cluster at a distance of ~ 310 pc, with a size $\sim 20'$ (Luhman 1999) and located in one end of the Perseus molecular cloud. Herbig (1998) found a significant spread in the age of the cluster (0.7 – 12 Myr) based on imaging observations in $BVRI$. Ground based JHK imaging by Lada & Lada (1995) revealed a central subcluster with a radius of 0.5 pc containing half the cluster members. Luhman et al. (1998) derived an age spread of 5 – 10 Myr for this subcluster which was confirmed by Najita et al. (2000). There have been

²<http://www-gsss.stsci.edu/gsc/gsc2/GSC2home.htm>

³Available from <http://www.ipac.caltech.edu/2mass/releases/second/index.html>

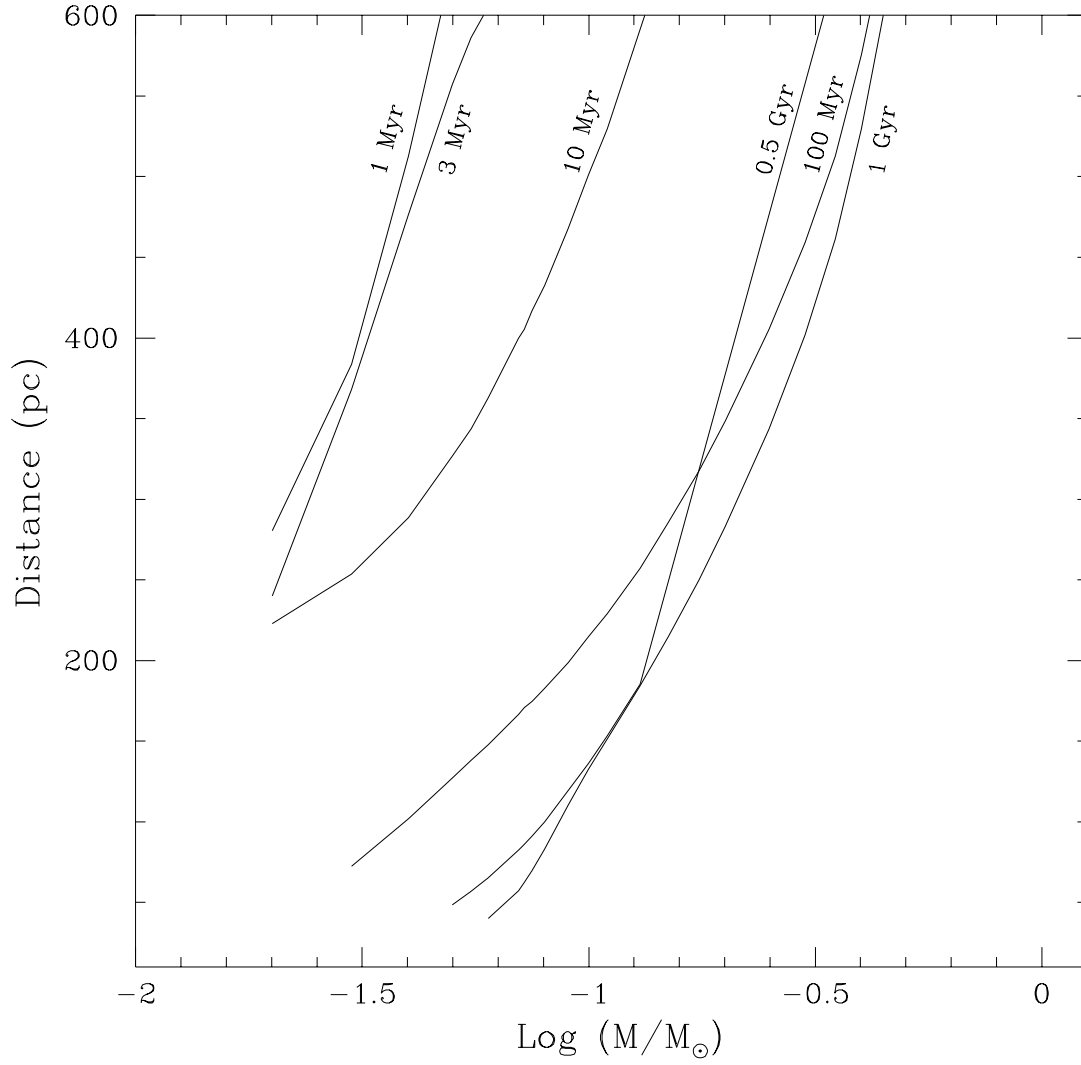


Fig. 2.— This figure shows the mass (in logarithmic units) as a function of distance for different isochrones derived for a limiting magnitude of 15 in the K band. The model isochrones are from Baraffe et al. (1998).

several surveys to detect and catalog the low mass members of this cluster (Luhman et al. 1998; Luhman 1999; Najita et al. 2000). Luhman et al. (1998) obtained infrared (K band) and optical spectroscopy and JHK photometry of the stellar population within the $5' \times 5'$ core of this cluster to study the star formation, disk properties and the mass function. In a continuing program to identify and characterize the low mass stellar and substellar populations in this cluster, Luhman (1999) carried out a wide and deep photometric survey in R and I covering a total area of $25' \times 25'$. Low resolution optical spectroscopy of a subset of the candidate substellar objects found from the survey was performed to confirm their membership. In conjunction with the evolutionary models of D'Antona & Mazzitelli (1997) and Baraffe et al. (1998), Luhman (1999) concluded that the HBML for this cluster occurs at a spectral type of M6 and that several objects found in the survey fall below the substellar boundary with masses as low as 20-30 M_J . Najita et al. (2000), using the *HST*/NICMOS narrow band imaging, investigated the low mass population down to the deuterium burning limit. Their study spans a mass range of $\sim 0.7 M_\odot$ to $0.015 M_\odot$.

3.2. σ Orionis

The Orion complex is one of the richest star forming regions in our Galaxy. *ROSAT* observations in the Orion belt led to the discovery of a large sample of X-ray sources near the bright young multiple star σ Orionis (Walter et al. 1994) which belongs to the Orion 1b association. Subsequent photometry and spectroscopy of the X-ray sources detected by *ROSAT* revealed the existence of a young stellar cluster (Wolk 1996). This cluster is located at a distance of 352 pc. The age of this cluster is in the range of 1 – 5 Myr (Béjar et al. 1999 and references therein) and its estimated size is $25'$ (Lynga 1983). Béjar et al. (1999) present the CCD observations in the R , I and Z bands covering a total area of 870 arcmin^2 around σ Orionis, which led to the detection of objects with masses down to $\sim 0.02 M_\odot$. By combining results from imaging surveys and follow up photometric and spectroscopic observations, Béjar et al. (2001) identified 64 very low mass members in this cluster, in the mass range $0.2 M_\odot$ to $0.013 M_\odot$. Barrado y Navascués et al. (2001b) have recently reported spectroscopic observations of planetary mass candidates in this cluster.

3.3. Pleiades

Pleiades is by far the best studied open cluster for low-mass stars. With an age of ~ 120 Myr and a distance of 125 pc, it is an ideal hunting ground for low mass stars and brown dwarfs. Imaging surveys to detect brown dwarfs began almost a decade ago (Jameson & Skillen 1989; Stauffer et al. 1989,1994; Simons & Becklin 1992; Rebolo et al. 1995; Cosburn et al. 1997; Zapatero Osorio et al. 1997,1999b; Bouvier et al. 1998; Festin 1998). Zapatero Osorio et al. (1997) reported the JHK' observations of some of the least luminous members of Pleiades and proposed a substellar limit at spectral type M7. In a deep IZ survey covering an area $\sim 1 \text{ deg}^2$ in the central region, Zapatero Osorio et al. (1999b) detected substellar candidates ranging in mass from $0.075 M_\odot$ to $0.03 M_\odot$.

Bouvier et al. (1998) performed a wide field imaging survey of the Pleiades cluster in the R and I passbands covering a large area of $\sim 2.5 \text{ deg}^2$ to a completeness limit of $R \sim 23$ and $I \sim 22$. They found 17 objects satisfying the criteria for brown dwarfs ranging in mass from the HBML down to $0.045M_{\odot}$.

4. The methodology

4.1. The data

As mentioned earlier, we have used the data from the 2MASS sky survey and the recently made available Guide Star Catalogue in this study. In selecting the 2MASS sources, we have constrained our sample to include only those sources for which the error in the K_s band is less than or equal to 0.15 mag to avoid the noisy data at the faint end. This would translate to a signal-to-noise ratio of ≥ 7 in K_s . This limit ensures positive detection in the other two bands as well. We have also taken into account the different flags so that our sample is not affected by the spikes of nearby bright stars, contamination from extended sources, or saturation in any of the three bands. Care is taken to exclude asteroids and minor planets, identified by the 2MASS catalog.

We merged the 2MASS data with the GSC sources by taking the 2MASS coordinates, and cross-correlating them with the GSC catalogue. For such a correlation, it is important to take an appropriate search radius which takes into account the uncertainty in the coordinates. The uncertainty in the coordinates mainly comes from the frame of reference used in the two catalogs. Comparison of Hipparcos data with the GSC data reveals that the GSC coordinates can differ by as much as $2''$ from the coordinates in the Hipparcos reference frame that 2MASS uses (Bakos, Sahu and Nemeth, 2002). A search radius of $2''$ was found to be an optimum value for this cross-correlation, which was small enough to reject spurious and multiple detections which could be the result of diffraction spikes due to bright stars in the field, and large enough to include any positional uncertainties in the two catalogs.

4.2. Initial selection of cluster members

Assigning cluster membership to sources is a difficult task. The color magnitude diagrams [CMDs] for various clusters given in the literature show that the density of faint members is usually comparable or even significantly less than the field/background/foreground population (Barrado y Navascués et al.(2001a) for IC 2391, Barrado y Navascués et al.(2001c) for M35 etc.) The use of CMDs can be used as an effective tool to delineate possible members from the field contaminants. Of course, proper motion and/or spectroscopic studies are needed to establish the membership of specific sources.

The CMDs best suited for this purpose can be determined by examining the locations of

sources with different masses and temperatures in different CMDs, and the slope and direction of the low-mass main sequence and the reddening vectors. An example K_s versus $(J - K_s)$ CMD is shown in Figure 3 where the dots represent the stars in the direction of the Pleiades cluster. To differentiate the line-of-sight contaminants from the cluster members we need a reliable locus for the low-mass main sequence.

These open clusters are located in the spiral arm of the Galaxy which comprises of the young disk population. To account for the contaminants, we construct a $K_s \sim (J - K_s)$ locus for the young-disk objects using the empirical data from Table 6 of Leggett (1992). The solid line in Fig. 3 shows such a disk sequence for all stars with spectral types M0 (corresponding to $0.5 M_\odot$) and later as taken from Leggett (1992). Here, we have appropriately shifted the Leggett sequence to take the distance and the extinction of the Pleiades cluster into account. The lowest two points in this line are identified as *young-old* (Y/O) by Leggett (1992). We derive the reddening vectors from the interstellar extinction laws of Rieke & Lebofsky (1980) and Bessell & Brett (1988); these reddening vectors are shown as dashed lines in the Fig. 3. We have chosen to plot the young-disk population because such a plot is likely to be most useful in rejecting the older non-member stars along the line-of-sight which are expected to fall to the left of this sequence owing to metallicity effects.

As seen from the figure, the stars with spectral types M0 and later fall more or less vertical in this diagram, and the $(J - K)$ color changes by ~ 0.35 over this entire spectral range. The reddening vector runs almost perpendicular to this sequence with a slope of ~ 0.67 . Since the effect of the distance is to move a particular source vertically in this diagram, there is a clear degeneracy between mass and distance for the mass range from $0.6 M_\odot$ to $\sim 0.06 M_\odot$ (Leggett 1992). For lower masses, the extinction vector runs almost parallel to the direction of the Leggett sequence creating a degeneracy between mass and extinction in this spectral range.

The inclusion of one optical color in the CMD [e.g. F versus $(F - J)$] overcomes the aforementioned degeneracies as explained below. One problem, however, is that the original data of Leggett (1992) give the absolute magnitudes and the intrinsic colors for the standard broad band filters in the Cousins, Johnsons and the CIT systems, and not in the F-passband. So we need to first convert the R magnitudes to F magnitudes by applying appropriate $(F - R)$ color corrections. For this purpose, we compared the Leggett young disk sequence with model isochrones of different ages in a F versus $(F - R)$ plot and found that the 100 Myr reasonably fits the Leggett young disk sequence as expected (e.g. Allen 1973). So we used the 100 Myr model isochrones in F and R to calculate the values of $(F - R)$, and applied this correction to the empirical R values derived from Leggett (1992). The resulting CMD in F versus $(F - R)$ is shown in Fig.4, where the color increases rapidly with spectral type (~ 3 mags) and the reddening vector is steeper with a slope of ~ 1.59 . Use of this plot avoids the degeneracies found in the $K_s \sim (J - K_s)$ CMD by minimizing the overlap between the reddened background stars and the low mass members of the cluster, and offers an efficient rejection criterion for non-members. Hence we have used the F vs. $(F - J)$ CMD to delineate field stars from the cluster members. Figure 4 shows a clear separation between the

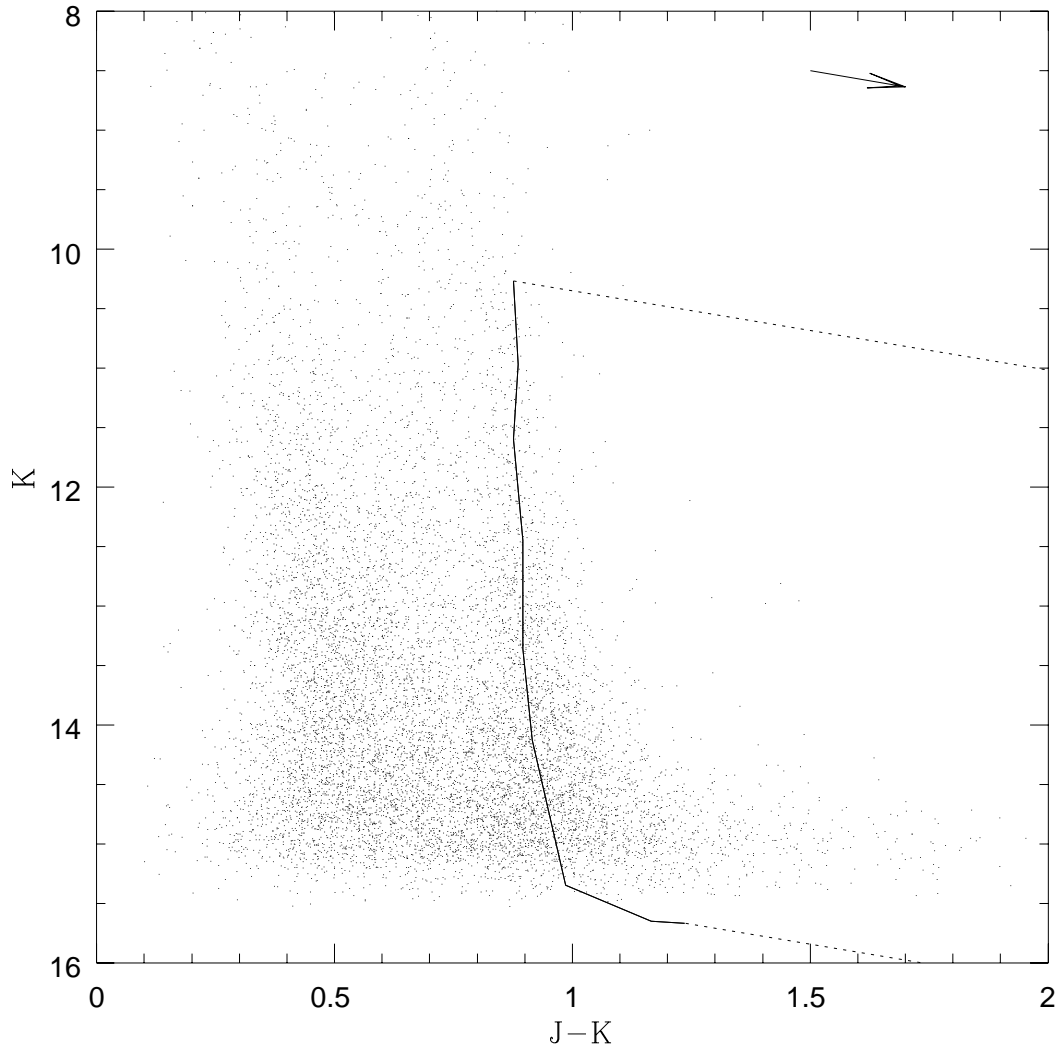


Fig. 3.— This figure shows the K_s versus $(J - K_s)$ plot for the Pleiades cluster. The Leggett main sequence is shown as the solid line from M0 and beyond. The dotted lines are the reddening vectors as derived from Rieke and Lebofsky (1985). The arrow indicates the direction of reddening.

cluster and non-cluster members, which justifies the use of this CMD.

While rejecting the field star population, care has to be taken not to reject genuine candidates from the sample. The disk population in the spiral arms are the field contaminants in the line-of-sight. As will be shown later, the main sequence from Leggett (1992), corresponding to this young disk population, falls to the left of the theoretical isochrones from Baraffe et al. (1998) for the clusters IC 348 and σ Orionis. Hence, this sequence from Leggett (1992) is preferred over the other for the rejection criterion for these two clusters. For the Pleiades cluster, which is ~ 100 Myr old, the two tracks overlap for most of the masses but the Baraffe model falls to the left for some part of the low mass sequence and hence is preferred over the Leggett main sequence to reject non members, and at the same time to ensure that none of the genuine members are rejected. Note that throughout the selection process, we have erred on the side of including some contaminants while ensuring that we do not reject *any* genuine low-mass objects. The price we pay in following this conservative approach is that our sample will inevitably include some foreground/background contamination. This is, however, a small price to pay since the contamination can be corrected through observations of the control fields. On the contrary, if some of the genuine objects are rejected, the effect can be disastrous since the observed number of stars would then be smaller than the actual number, thus making the statistics potentially incorrect. It is worth noting here that, since we have followed this conservative approach, the sources lying between the Leggett main sequence and the theoretical isochrone should be treated with caution.

Even though the F vs. $(F - J)$ CMD is a better choice to separate the cluster members from the non-members, we still see a smooth transition between the field stars and the cluster members in Fig. 4 which implies that our cluster sample would still be contaminated. This contamination could be due to the background reddened stars as well as the foreground population. We need to correct for this contamination before we can derive a reliable mass function. This becomes especially important in our study since we are not carrying out follow-up spectroscopic or proper motion studies to confirm the membership of individual members. As we will demonstrate in detail later, the contamination can be satisfactorily taken into account by studying the properties of off-fields or control fields in the vicinity of the clusters. We have tried to use several control fields, each covering the same area as the cluster, which are located near the cluster and are free from anomalies. These control fields were selected by visually inspecting the star density from the POSS plates. For IC 348, we have used the CO maps of Bachiller & Cernicharo (1986) to find suitable control fields. Table 2 gives the location and sizes of the cluster and control fields used in our study.

4.3. Stellar mass determination

The masses of our selected candidates are determined by comparing the observed magnitudes with those predicted by the evolutionary models. We have used the evolutionary tracks of Baraffe et al. (1998) for this purpose, as they provide the magnitudes and colors as a function of mass for various ages in the passbands of interest. The magnitudes in the F-bands were specially calculated

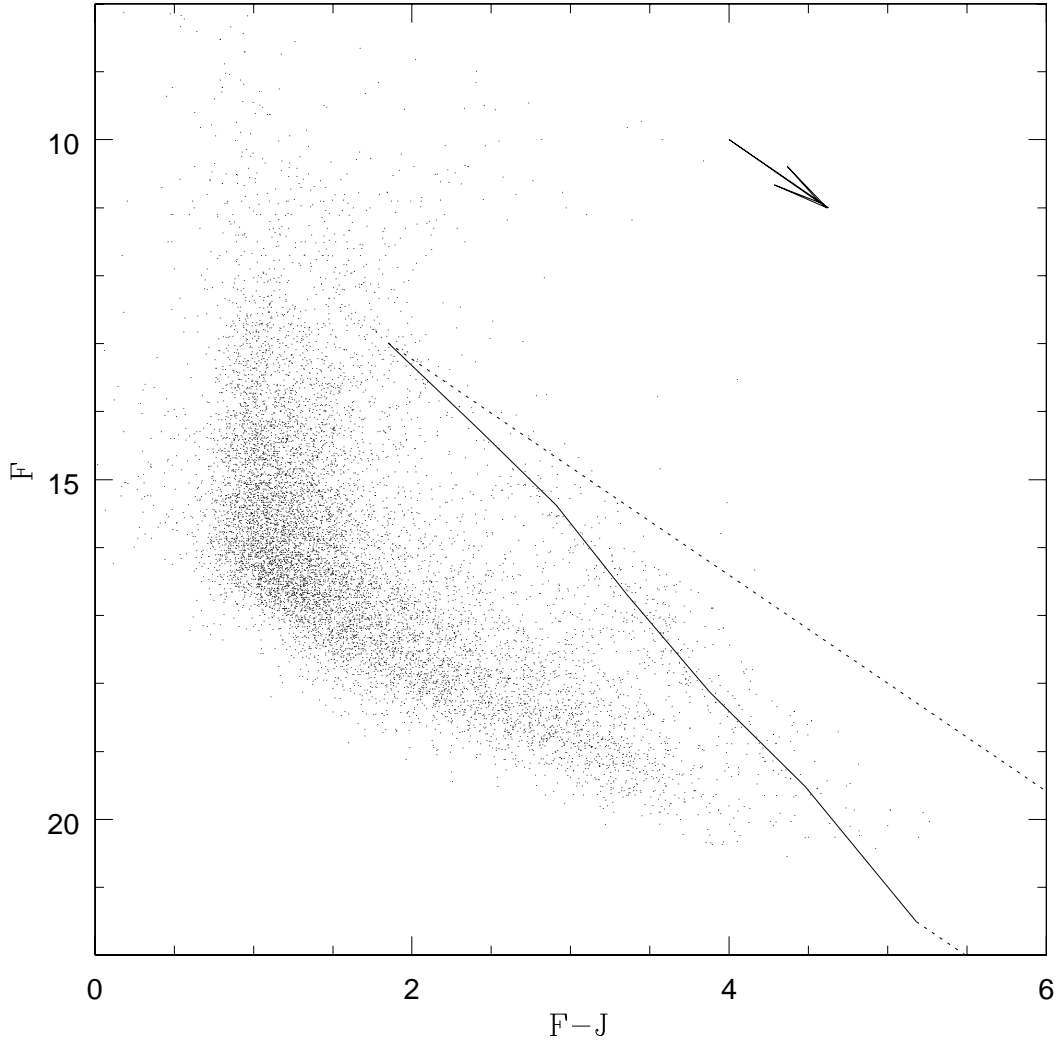


Fig. 4.— Same as Fig. 3 showing the F versus the $(F - J)$ plot.

and were kindly provided to us by Baraffe and Allard at our request, which are used in this analysis. Whereas, in order to transform the effective temperatures and luminosities of other models we need to use the bolometric corrections of the Baraffe model. Additionally, the tracks by Baraffe et al. (1998) have been successful in fitting the mass-luminosity relation in various optical and infrared passbands and predicting coeval ages for members of several young multiple systems (White et al. 1999; Luhman 1999). It is also seen that these models provide good fits to the infrared photometric sequence in the Pleiades and σ Orionis clusters (Martín et al. 2000; Zapatero Osorio et al. 2000). It is worth emphasizing here that the mass determinations are model dependent and are subject to possible systematic effects arising from the different parameters used in the models.

5. Low mass members and the mass function

In this section we discuss the selection criteria and the resulting mass functions derived for the individual clusters.

5.1. IC 348

To sample the entire cluster, we consider all the sources within a radius of $20'$ around the cluster center of IC 348. The wide and deep study of Luhman (1999) also covers almost the entire cluster, and includes optical photometry and follow-up spectroscopy. The study by Luhman et al. (1998) includes both optical and near-IR observations for the central $5' \times 5'$ of the cluster. Since our study includes both optical and near-IR photometry, IC 348 provides an ideal opportunity to compare the results, and to check the consistency between the different approaches. For this cluster, we derive the value of interstellar reddening from the sample of 70 confirmed low mass cluster members of Luhman (1999). The observed distribution of the extinction values listed in Luhman (1999) ranges from $A_V = 0.0$ to $A_V \sim 8$ with a peak around $A_V=0.3$ magnitudes. We have used the lower value of $A_V = 0$ magnitudes in our selection criteria to ensure that none of the genuine cluster members are rejected. The fact that some members of IC 348 have zero extinction is also seen in the data of Najita et al. (2000) where there are a few sources with $A_K = 0.0$.

Fig. 5 shows the F versus $(F - J)$ plot for all the sources in this region of the cluster and the two control fields. The figure also shows the main sequence from Leggett (1992) and the theoretical isochrone for 5 Myr from Baraffe et al. (1998) appropriately scaled to a distance of 316 pc (Herbig 1998) and an interstellar reddening of A_V of zero.

The number of sources increases to the left of the main sequence locus which can be attributed to the field star contamination. Hence, the objects bluer and fainter than the Leggett main sequence are rejected, giving us the first criterion for the choice of candidates, which is derived by fitting a

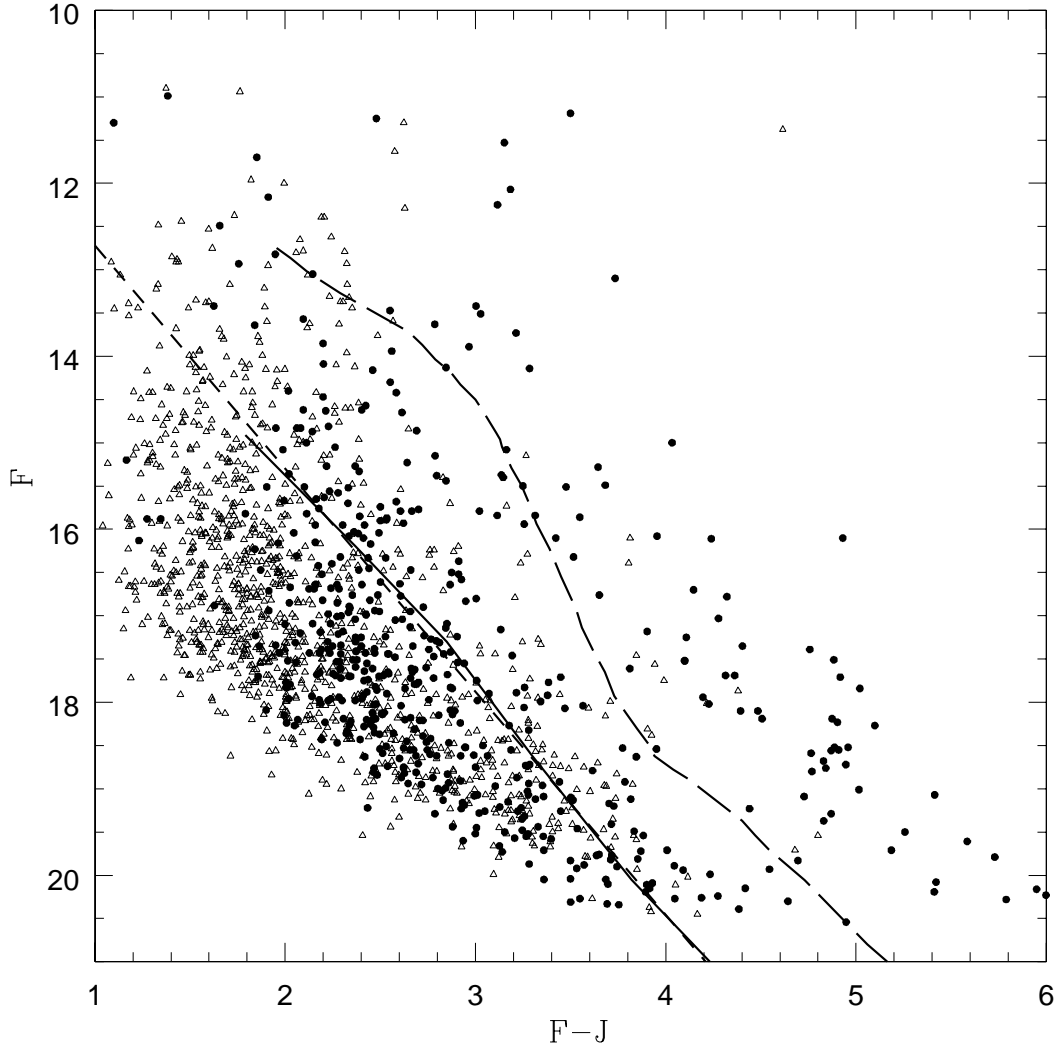


Fig. 5.— The F versus the $(F - J)$ plot for IC 348 (closed circles). Also plotted are the sources from the control fields (open triangles), the Leggett main sequence (solid), the straight line fit to the Leggett main sequence (short dashed) and the 5 Myr isochrone from Baraffe et al. (1998) (long dashed). For clarity we have plotted every second point of the cluster and the control fields.

straight line to the data points of Leggett (1992)

$$F < 2.58(F - J) + 10.14 \quad (3)$$

We then use the model isochrones from Baraffe et al.(1998) in other CMDs appropriately scaled to the distance and extinction of IC 348, to select the low mass members of the cluster. As discussed in section 3.1, this cluster exhibits appreciable spread in the age. We adopt a mean age of 5 Myr and use the magnitudes and colors of the Baraffe models to formulate the following criteria for selecting the objects with mass $< 0.5M_{\odot}$.

$$F - K \geq 4.09 \quad (4)$$

$$K \geq 11.20 \quad (5)$$

$$J - K \geq 0.90 \quad (6)$$

$$H - K \geq 0.20. \quad (7)$$

The sources satisfying all the four criteria are designated as potential low-mass members of the cluster and the sources in the control fields which satisfy these criteria are used to correct for the possible contaminants. Fig. 6 shows the K_s versus $(J - K_s)$ plot of the sources satisfying the low mass selection criteria. The closed circles represent the sources from the cluster and the open triangles are the candidates from the control fields which represent the possible contaminants. The plot also shows the theoretical isochrone for a 5 Myr cluster scaled to the distance and reddening of IC 348. As one can see, there are a few sources from the control samples to the right of the theoretical isochrone. We correct for this contamination while deriving the mass function. Also plotted are the confirmed low mass members from the Luhman (1999) sample (open circles). The fact that they all fall in the region satisfying all our selection criteria proves the validity of this approach. This figure also suggests low internal extinction in this cluster. If the internal extinction were high, the stars in the near side of the cluster would undergo less extinction, and the stars on the far side would undergo more extinction. As a result, the observed stars would be expected to fall on both sides of this theoretical main sequence. Thus, the fact that very few stars lie to the left of the main sequence implies that most of the extinction must be foreground rather than internal. On the other hand, we do observe many stars on the right side of the theoretical sequence. Since the internal extinction is not large, this would argue that the most of the observed extinction is not interstellar, but circumstellar. In a recent work Muench et al. (2001) find, from the analysis of the JHK colors, that $\sim 50\%$ of the brown dwarf candidates in the Trapezium cluster display significant infrared excess. This suggests that these sources are extremely young and provides independent confirmation of their cluster membership and low mass nature. Fig. 7 shows the $(J - H)$ versus $(H - K)$ color - color diagram for the low mass stars of the cluster and the control fields. In this figure, the region to the left of the reddening band is forbidden for young stellar objects. Hence, the location of sources in this region is most likely due to the combined uncertainties in the models,

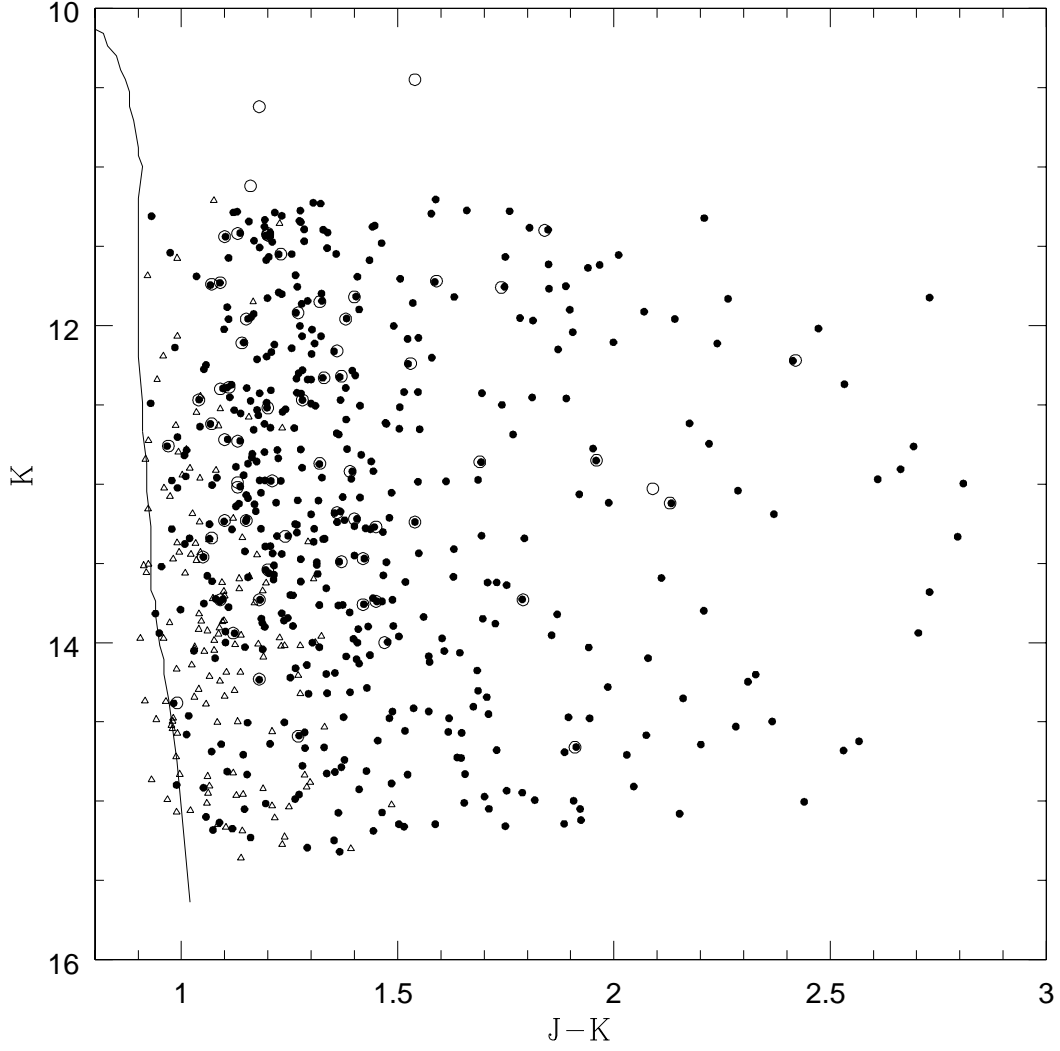


Fig. 6.— The K_s versus $(J - K_s)$ diagram for the sources satisfying the low mass criteria, IC 348 (closed circles) and control fields (open triangles). Also plotted is the theoretical isochrone of 5 Myr from Baraffe et al. (1998)(solid line). This plot also shows the position of the confirmed low-mass members of this cluster from Luhman (1999)(open circles).

the derived magnitudes and the extinction characteristics. The region to the right of the reddenning band is occupied by sources with infrared excess (Lada & Lada 1995). This is in agreement with the discussion on the circumstellar extinction.

To derive the mass function, we construct mass bins of $0.01 M_{\odot}$ in the mass range $0.02 - 0.09 M_{\odot}$. As the number of candidates decreases for higher masses, the width of the bin is increased to $0.1 M_{\odot}$ for the mass range $0.1 - 0.5 M_{\odot}$. The members of the cluster field and the two control fields satisfying the five selection criteria are grouped into these mass bins. The grouping is done based on the model-predicted K magnitudes for these mass bins taking the distance, age and mean extinction of IC 348 into account. The number of sources in each mass bin is then normalized with the total number of sources detected in that field. This is essential in order to correct for the unequal area covered by the cluster and the control fields, often caused by incompleteness of the survey. The mean percentage of the number of sources present in each mass bin of the control fields quantifies the contamination one expects. This percentage contamination is then removed from the cluster bins and divided by the bin width to obtain the value of dN/dM . This as a function of the mass gives the mass function (Eqn 1 & 2). Fig. 8 shows the resultant mass function for IC 348. The closed circles are based on the models of Baraffe et al. (1998) and the open triangles are derived using the models of Chabrier et al. (2000) which include dust opacities. The error bars in y show the \sqrt{N} errors involved in the counting statistics. The least squares fit to the data points derived from the Baraffe et al. (1998) model yield a slope of $-0.7(\alpha = 0.7)$, with an uncertainty of ± 0.2 . In deriving this slope, we have rejected the lowest mass bin since this is affected by the limiting magnitude of the 2MASS survey. As seen from this figure the results from the models of Chabrier et al. (2000) are in agreement with the non-dusty models of Baraffe et al. (1998) within the given scatter.

The mass function derived here is consistent with that derived by Najita et al. (2000) and Luhman et al. (1998). Using the tracks from D’Antona & Mazzitelli (1997), Luhman et al. (1998) derive a mass function which, in logarithmic units, slowly rises from the HBML to $\sim 0.25 M_{\odot}$ with a slope of ~ -0.4 . Converting their results to our system (Eqn. 1 & 2) yields a value of $\alpha = 0.6$. Najita et al. (2000) derive the mass function using the models of Baraffe et al. (1998) as well the evolutionary tracks of D’Antona & Mazzitelli (1997). They derive mass functions with $\alpha = 0.5$ and $\alpha = 0.4$ respectively for the two models.

5.2. σ Orionis

We have assumed a mean age of 3 Myr from the age estimates of Béjar et al. (1999) for σ Orionis. Lee (1968) finds a low extinction of $E(B - V) = 0.05$ for the multiple star σ Orionis which suggests that the reddening of the associated cluster is small. We also assume this value of $E(B - V)$ in our analysis as the value of the foreground extinction for the cluster. We have covered an area of $\sim 0.8 \text{ deg}^2$ centered around the star σ Orionis. Taking the distance to be 352 pc (Béjar et al. 1999), we derive the following criteria for field star rejection and selection of low

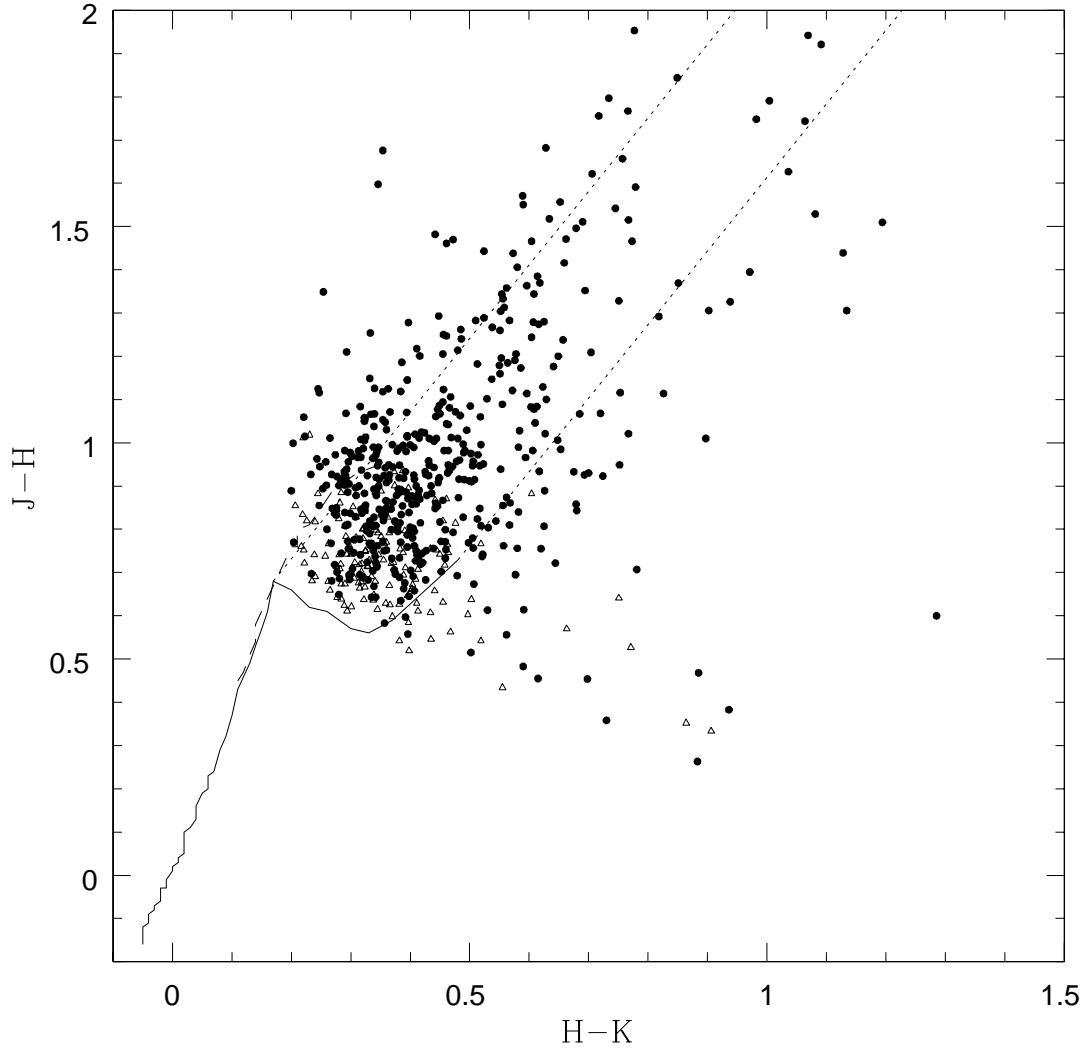


Fig. 7.— The $(J - H)$ versus the $(H - K_s)$ color - color plot for IC 348 (closed circles) and the control fields (open triangles). The solid and the dashed lines are the main sequence and the giant sequence from Koorneef (1993). The dotted lines are the reddening vectors derived from Rieke & Lebofsky (1980).

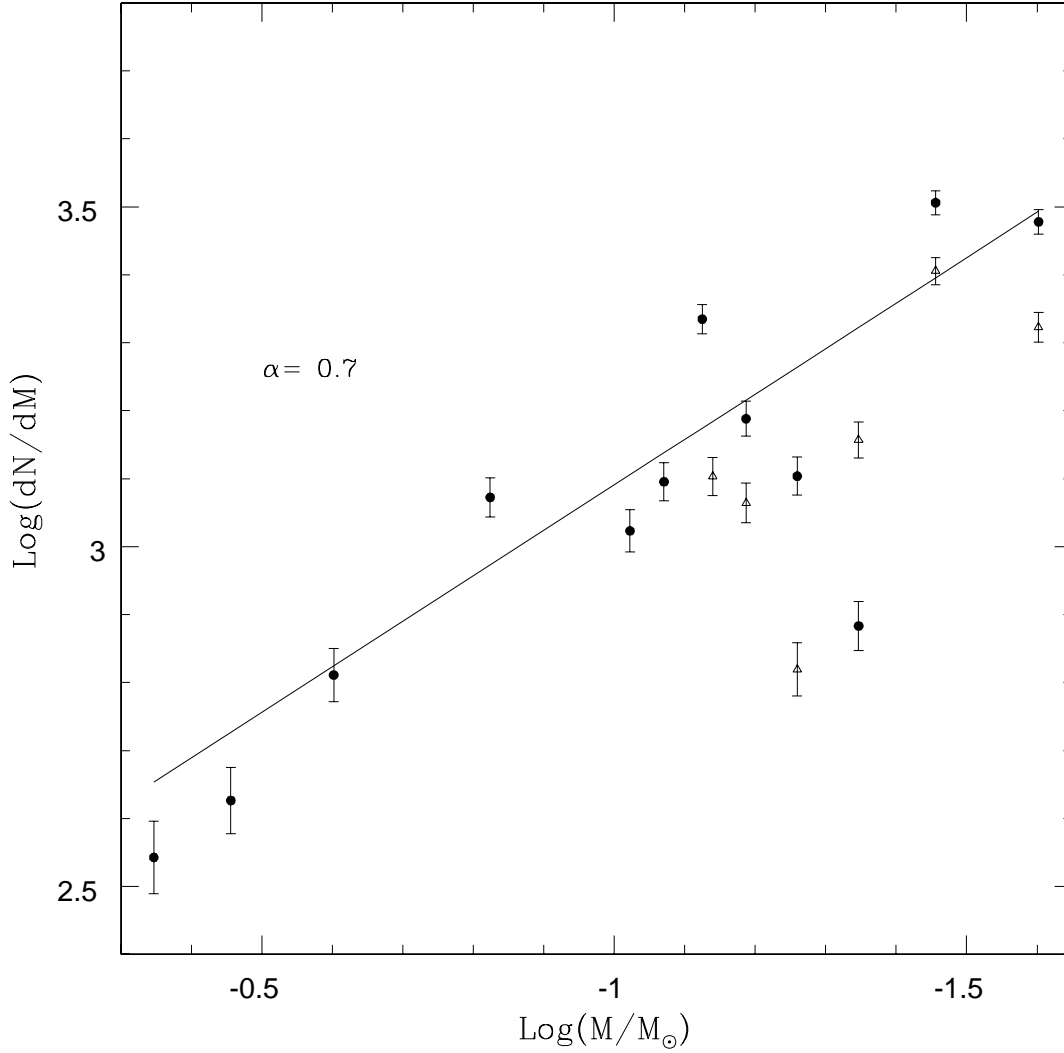


Fig. 8.— The mass function derived for IC 348. The y-error bars are the \sqrt{N} errors of the counting statistics. The filled circles are data points derived using the models of Baraffe et al. (1998) and the open triangles represent data points from the models of Chabrier et al. (2000). This figure also plots the least squares straight line fit to the data points.

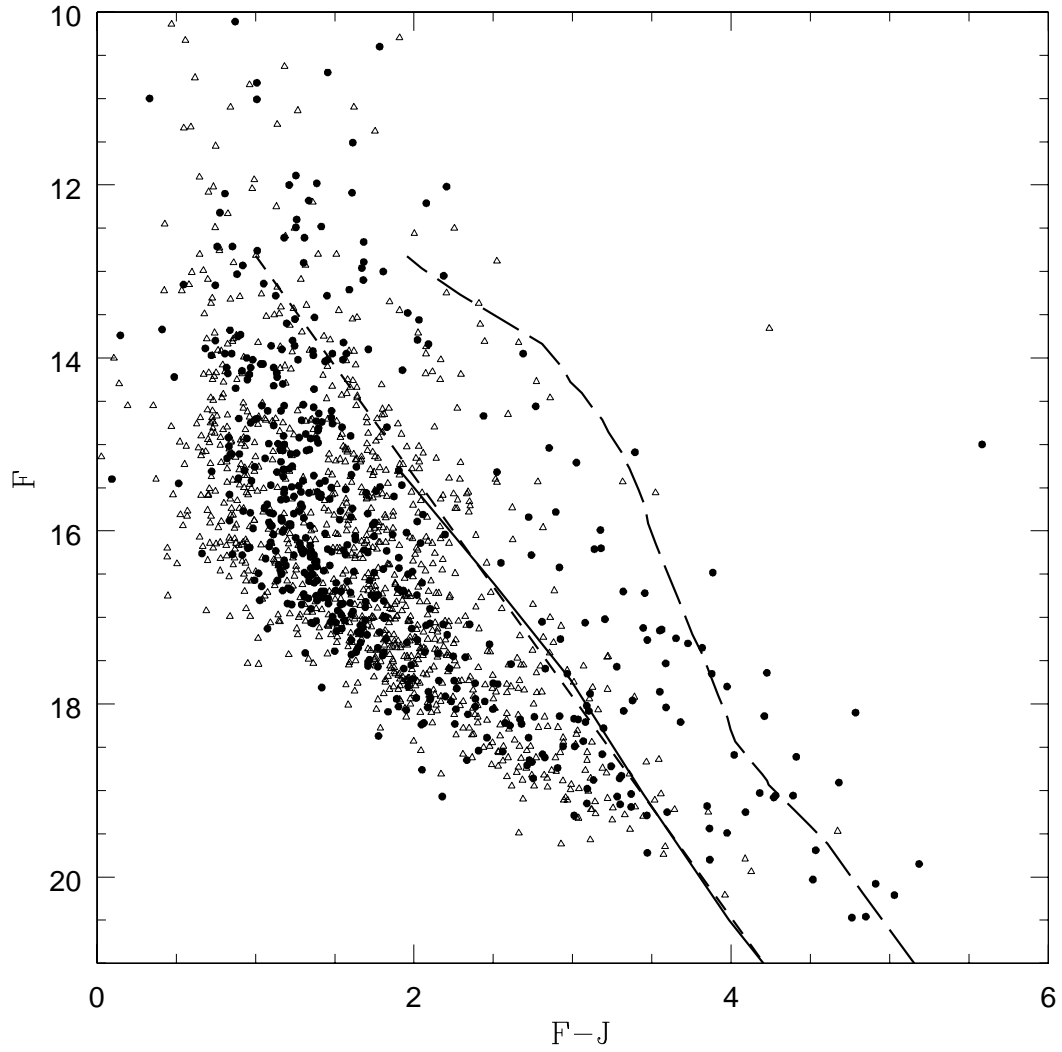


Fig. 9.— Same as Fig. 5 but for σ Orionis showing every fifth point of the cluster and the control sample. Here, the plotted isochrone is for 3 Myr from Baraffe et al. (1998).

mass members

$$F < 2.55(F - J) + 10.26 \quad (8)$$

$$F - K \geq 4.35 \quad (9)$$

$$K \geq 11.17 \quad (10)$$

$$J - K \geq 0.94 \quad (11)$$

$$H - K \geq 0.20. \quad (12)$$

Fig. 9-11 show the different CMDs and color-color plots for σ Orionis. As is evident from the figures, the contamination for this cluster is higher than that of IC 348. The possible reason might be the location in the Orion Complex and inadequate correction for variable extinction in the cluster and the control field.

The derived mass function is shown in Fig. 12. As seen in the figure there is a sudden rise in the mass function at $0.045 M_{\odot}$, which could be because of the large contamination from the background sample. The lowest mass bin is affected by the limiting magnitude of the survey. Hence, these two lowest mass bins were excluded in deriving the slope of the mass function. The resultant mass function has a slope of $\alpha = 1.2 \pm 0.2$. Béjar et al. (2001) have previously derived the mass function for this cluster in the mass range from $0.2 M_{\odot}$ to $0.013 M_{\odot}$ based on deep photometry in I,Z,J and K bands. They obtain a slope of $\alpha = 0.8 \pm 0.4$ assuming the age to be 5 Myr. Our study, which covers a larger area and includes photometry in all the 2MASS near-IR bands, is consistent with the results of Béjar et al. (2001).

5.3. Pleiades

For Pleiades, we have selected four fields of 1 deg radius each and centers offset by a degree from the cluster center towards the north, south, east and west. These four fields are then combined together to one field with an effective radius of 1.5 deg centered around the cluster center and hence amounts to a total area of $\sim 7 \text{ deg}^2$. In contrast to many of the previous studies, our study thus covers a large area and includes the photometry in optical as well as the near-IR wavelengths. The control fields are generated in similar fashion. As compared to IC 348 and σ Orionis, Pleiades is an older cluster with an age estimate varying between 100 – 125 Myr. In our analysis, we assume an age of 100 Myr (Bouvier et al. (1998), a distance of 125 pc (Bouvier et al. 1998) and a redenning of $A_v=0.12$ (Crawford & Perry 1976) for the cluster. Fig. 13 shows the F versus the $(F - J)$ diagram for Pleiades. Because of the high galactic latitude of this cluster one sees a better separation between the field and the cluster members unlike that in the other two clusters. As explained in section 4.2, we have used the locus of the Baraffe model to set a criterion for rejection of the field population. A 4th order polynomial best fits the theoretical isochrone for a 100 Myr cluster.

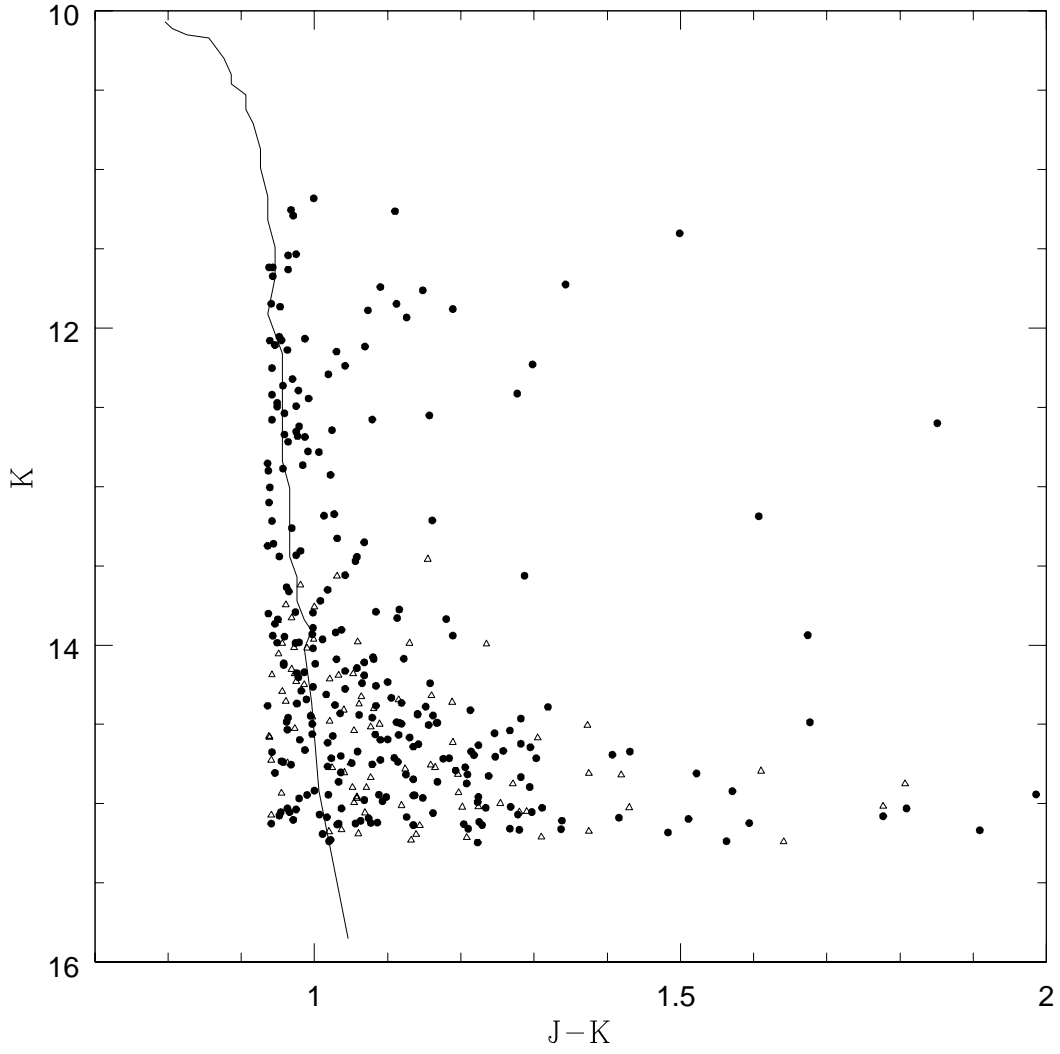


Fig. 10.— Same as Fig. 6 but for σ Orionis.

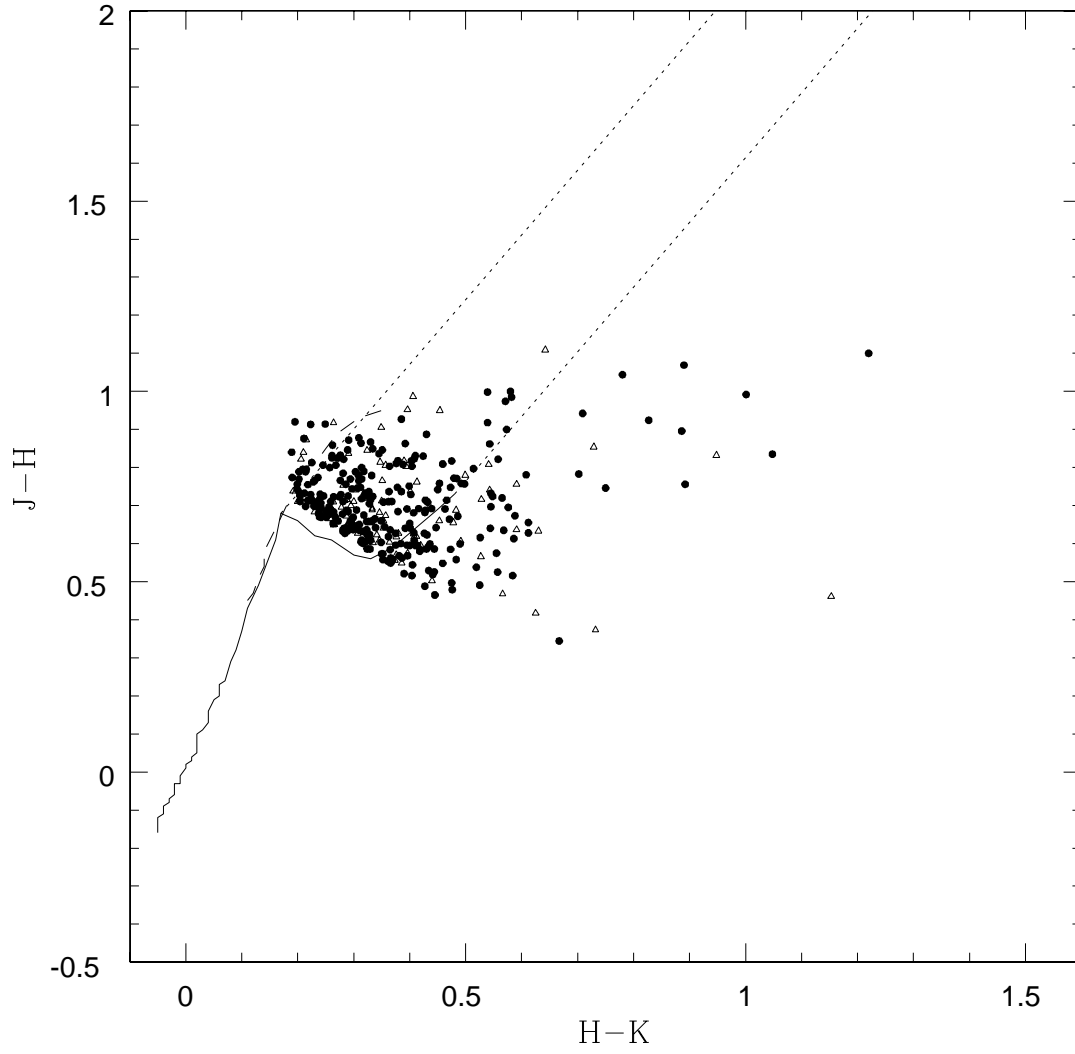


Fig. 11.— Same as Fig. 7 but for σ Orionis.

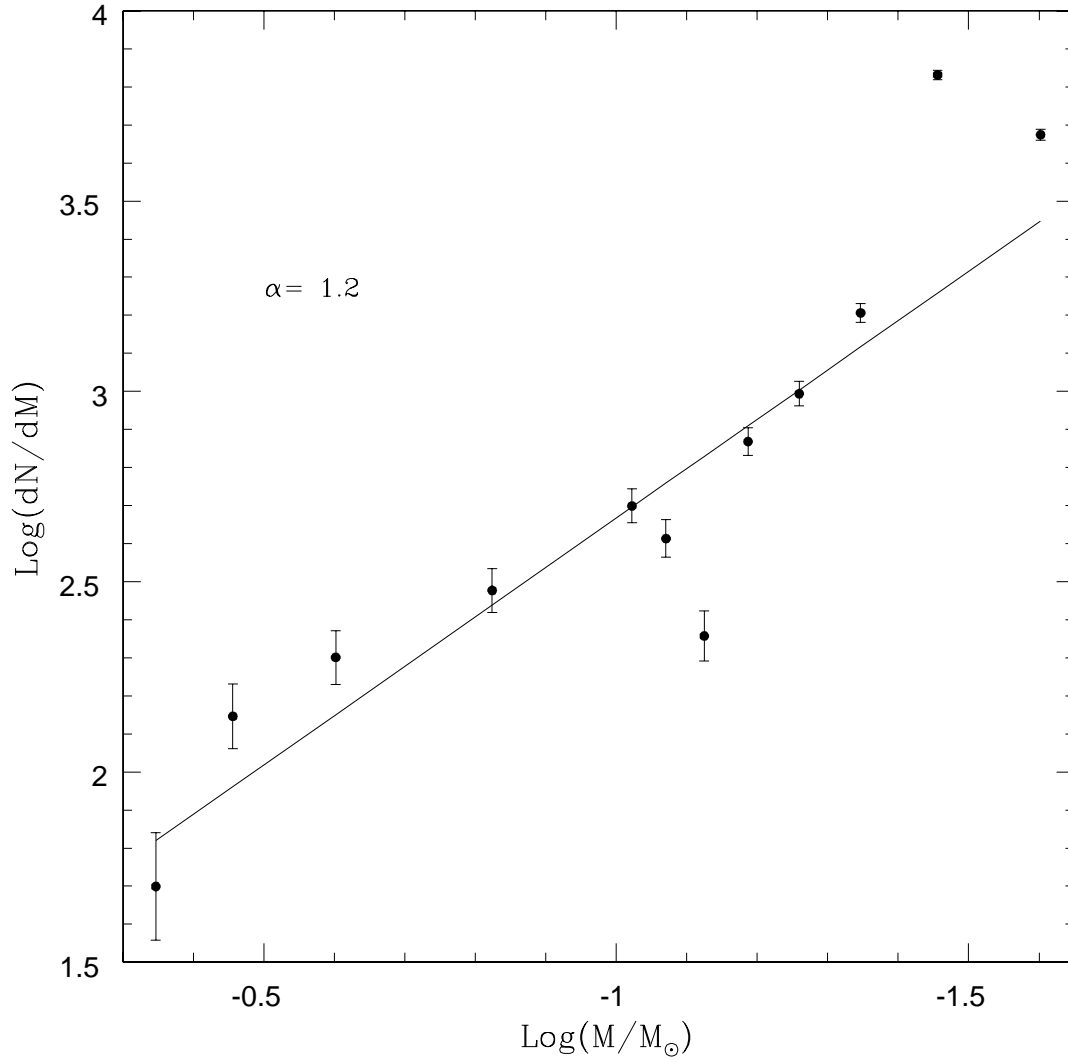


Fig. 12.— The mass function derived for σ Orionis.

The other criteria are derived analogous to the previous two clusters. The resultant criteria are as follows.

$$F < 7.93 + 1.99(F - J) + 0.56(F - J)^2 - 0.13(F - J)^3 + 0.01(F - J)^4 \quad (13)$$

$$F - K \geq 3.42 \quad (14)$$

$$K \geq 11.17 \quad (15)$$

$$J - K \geq 0.83 \quad (16)$$

$$H - K \geq 0.22 \quad (17)$$

Fig. 13-15 show the color – magnitude and the color – color plots for Pleiades.

Fig. 16 shows the derived mass function. The linear fit to the data points yields a value of $\alpha=0.5$. This is in good agreement with the results of Bouvier et al. (1998) who derive a mass function which still rises below the HBML with $\alpha=0.6$. Martín et al. (1998), from a compilation of independent photometric survey covering different areas of the cluster, derive a steeper slope in the mass range $0.04 - 0.25 M_{\odot}$ with $\alpha=1.0\pm 0.15$. Hambly et al. (1999) derive a value of $\alpha=0.7$ from a R and I survey covering an area of 6×6 degrees centered on Pleiades. It is worth noting here that Pleiades is a relatively older cluster, where the mass segregation and the escape mechanism of low-mass stars described earlier might have played a role. This may be the reason for the flatter slope compared to the other two clusters, and may also also explain the observed discrepancies in various estimates of the slopes indicating that the mass function may not be uniform over the entire region of the cluster.

6. Discussion and Conclusion

Recent surveys have found a significant population of low mass stars, brown dwarfs and planetary mass objects in young open clusters. We have adopted a statistical approach to determine the mass spectrum, $dN/dM \propto M^{-\alpha}$, of objects in the mass range $0.5M_{\odot}$ to $0.025-0.055M_{\odot}$, using the data from the recently released 2MASS and the GSC catalogues. Unlike some of the previous studies, our study makes use of both the optical data as well as the near-IR data. Since these datasets cover a large portion of the sky, they allow us to study the entire area covered by each cluster. As a result, the areas covered in our study are generally larger than the areas covered in most of the previous studies. These datasets also allow us to apply a statistical approach to efficiently subtract the background contribution using several control fields close to the cluster.

We carried out a detailed study for IC 348. For this cluster, we derived the mass functions using the solar metallicity model of Baraffe et al. (1998) and the dusty models of Chabrier et al. (2000), both of which gave very similar results. We also compared the confirmed low-mass members from Luhman (1999) with our isolated low-mass candidates which further strengthened the validity of

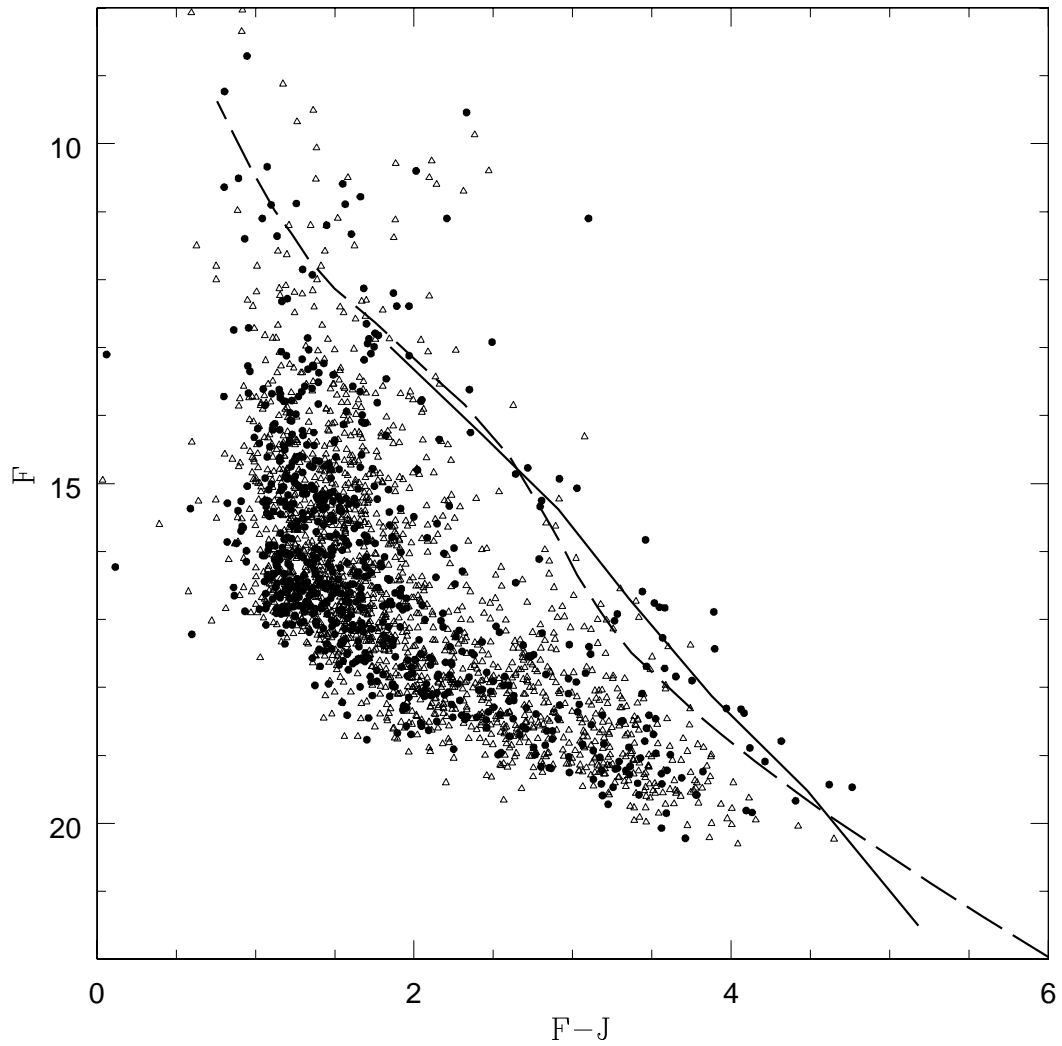


Fig. 13.— Same as Fig. 5 but for Pleiades showing every fifteenth point of the cluster and the control fields. The model isochrone here is for 100 Myr and the fit to this model isochrone is given by Eqn. 13.

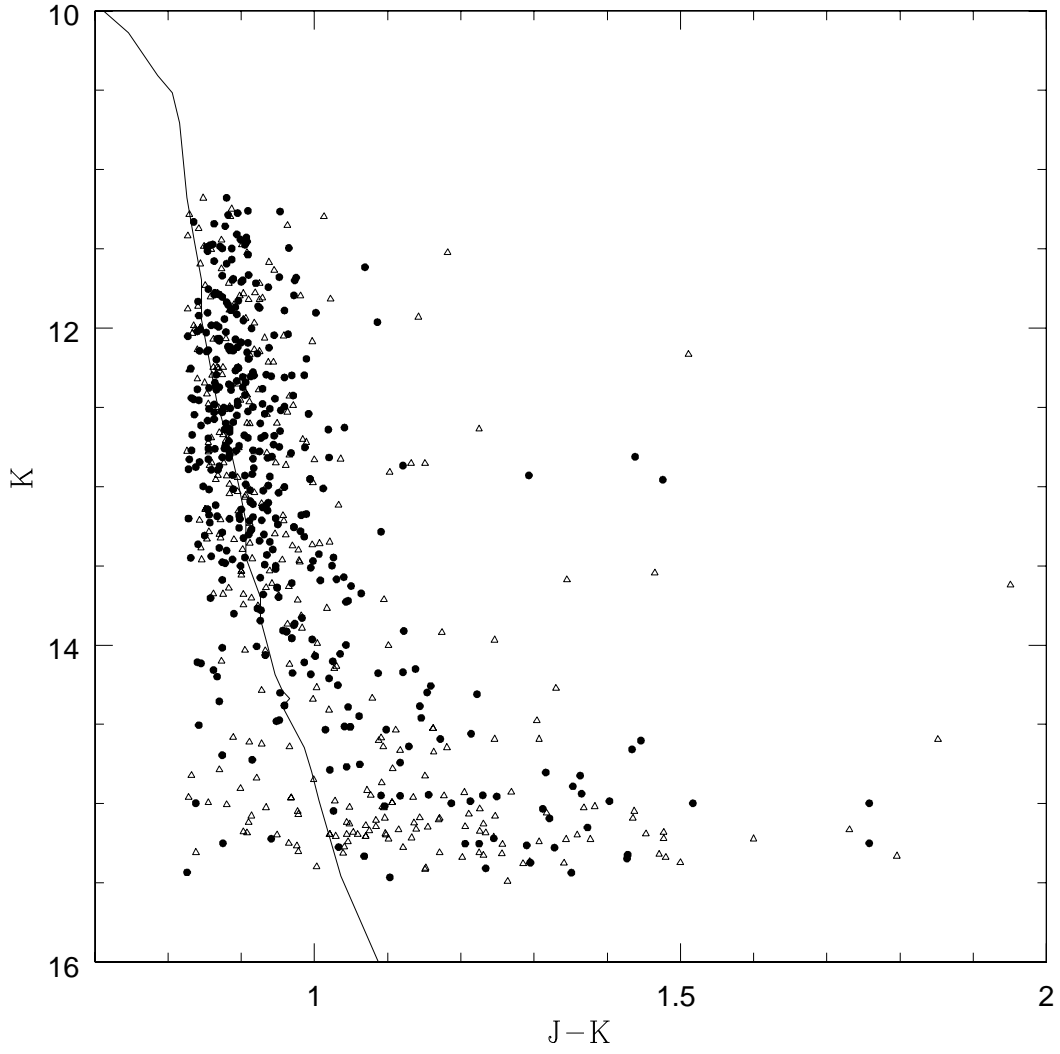


Fig. 14.— Same as Fig. 6 but for Pleiades.

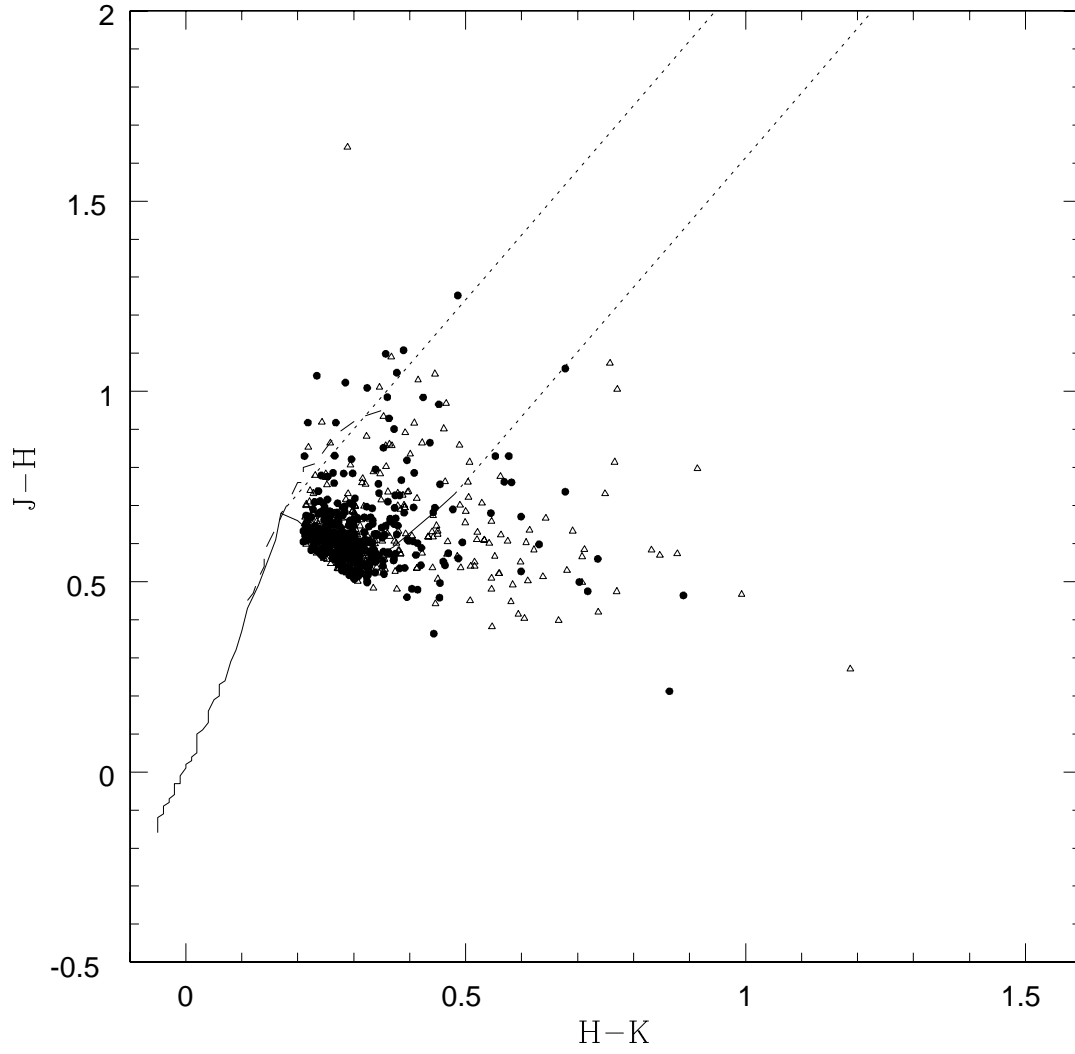


Fig. 15.— Same as Fig. 7 but for Pleiades.

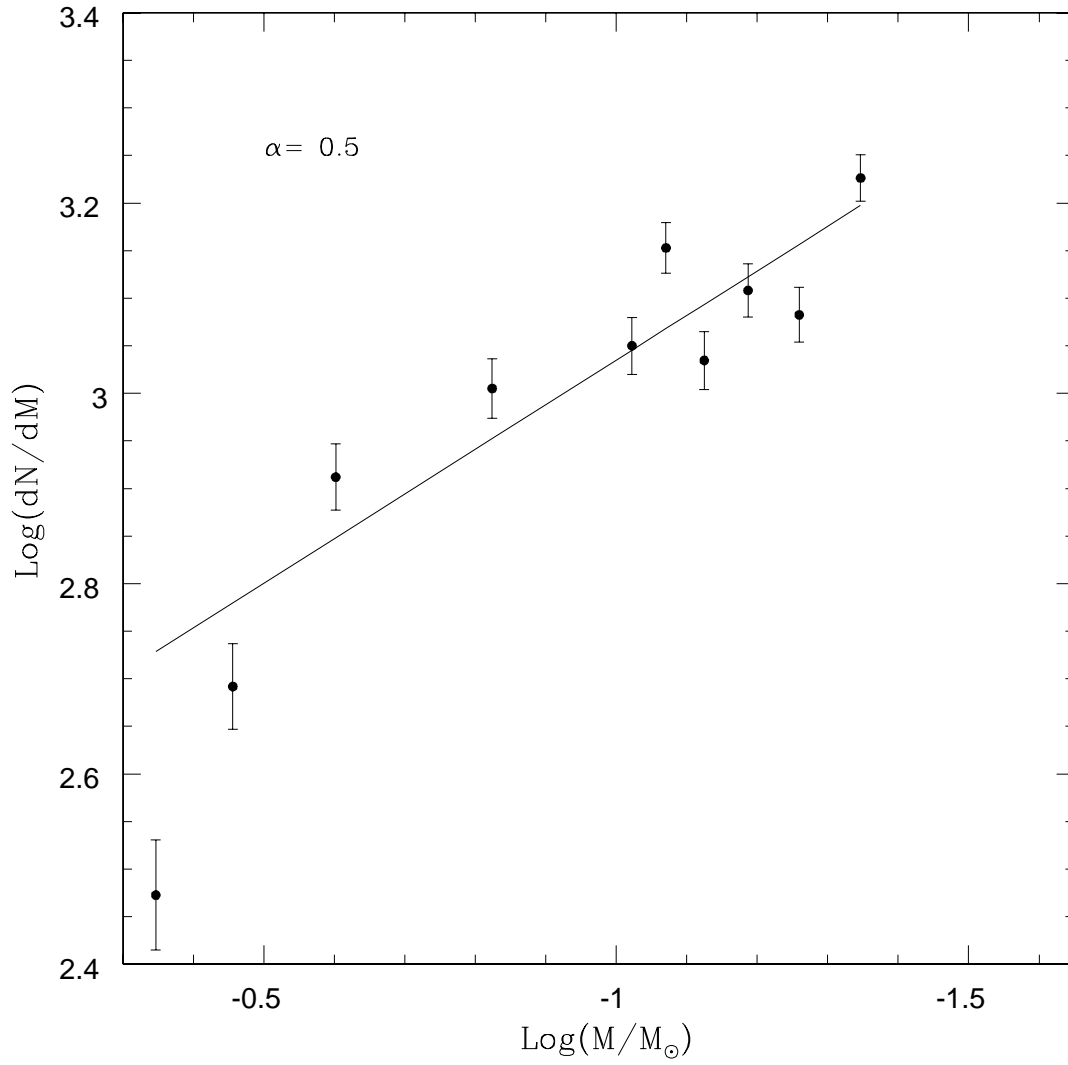


Fig. 16.— The mass function derived for Pleiades.

this technique. We then used the same technique to σ Orionis and Pleiades. The resultant slopes of the mass functions for IC 348, σ Orionis and Pleiades are 0.7, 1.2 and 0.5 respectively, with an estimated error of ± 0.2 . For IC 348 we have used the mass range from $0.5M_{\odot}$ to $0.025M_{\odot}$ in deriving the slope of the mass function whereas for *sigma* Orionis and Pleiades, the lowest mass bins correspond to $0.045 M_{\odot}$ and $0.055M_{\odot}$, respectively. Taking into consideration the effect of mass segregation and preferential loss of low mass members from the cluster, the mass function derived here for the inner 1.5 deg radius of Pleiades cluster could be considered as a lower limit to the true mass function. As discussed under individual sections, the mass functions derived here are in good agreement with the value derived by other groups based on studies of confirmed low mass members of these clusters, which demonstrates the consistency of different approaches. Within the uncertainties, the values of α derived for the IC 348 and σ Orionis is in agreement with that derived for the local sample of low-mass stars (Reid et al. 1999). The derived slopes imply that the mass spectrum continues to rise well below the HBML, but the mass functions are appreciably flatter in the low-mass regime than the Salpeter mass function. The results are summarized in Table 3.

Taking the Salpeter exponent of 2.35 in the mass range $1 - 10 M_{\odot}$, the Chabrier exponent of 1.55 in the mass range $0.5 - 1 M_{\odot}$, and the values obtained by us below $0.5 M_{\odot}$, we calculate the mass contribution to be about 40% for objects below $0.5 M_{\odot}$, and about 4% for objects below the HBML of $0.08 M_{\odot}$. (Note that the contributions are not sensitive to the choice of the slope in the higher mass regime. For example, if we use the value of α as 2.7 for $M > 1M_{\odot}$ as derived by Chabrier (2001) instead of the Salpeter value of 2.35, the mass contributions change only by $\sim 1\%$). Our results are consistent with that of the previous studies (e.g. Béjar et al. 2001), and suggest that, although the low mass stars are at least as numerous as their high mass counter parts (as seen from figures 5,7 and 9), their contribution to the total mass is small. The contributions of low-mass objects to the total mass in the clusters seem to be marginally smaller than that of the low-mass objects in the local sample (e.g. Reid et al. 1999), but the slope of the mass function is less steep for the relatively older Pleiades cluster. This is not surprising since the high-mass stars are likely to be preferentially lost in an older and mixed population such as the local sample.

Follow up spectroscopic observations to confirm the isolated low mass members of the clusters would further strengthen the results derived from this purely statistical approach.

acknowledgements

We would like to thank Brian McLean and Mario Lattanzi (the GSC-II project scientists) for access to the development version of GSC-II in advance of publication and their technical comments. We would like to thank the anonymous referee for valuable comments and suggestions. We are grateful to I. Baraffe and F. Allard for making the electronic versions of the latest models available and generating the model isochrones for the non-standard F passbands. We would also like to thank Neill Reid for useful discussions. The visit of A. Tej to STScI was supported by a DDRF grant of STScI awarded to K. Sahu. The Digitized Sky Surveys and the Guide Star Catalogues were

produced at the Space Telescope Science Institute under US Government grant NAG W-2166; the images of these surveys are based on photographic data obtained using the Oschin Schmidt Telescope on Palomar mountain and the UK Schmidt Telescope at Siding Spring. The 2MASS project is a collaboration between The University of Massachusetts and the Infrared Processing and Analysis Center (JPL/ Caltech), the funding for which is provided primarily by NASA and the NSF. Research work at PRL is funded by Dept. of Space, Govt of India.

REFERENCES

- Adams, F.C., & Fatuzzo, M. 1996, *ApJ*, 464, 256
- Allen, C. W 1973, *Astrophysical Quantities*, Univ. of London The Athlone Press, p242
- Allard, F., Hauschildt, P.H., Baraffe, I., & Chabrier, G. 1996, *ApJ*, 465, L123
- Bachiller, R., & Cernicharo, J. 1986, *A & A*, 166, 283
- Bakos, G.A., Sahu, K.C., & Németh, P. 2002, *ApJ Suppl.* (in press) (astro-ph/0202164)
- Baraffe, I., Chabrier, G., Allard, F., & Hauschildt, P.H. 1998, *A & A*, 337, 403
- Barrado y Navascués, D., Stauffer, J.R., Briceño, C., Patten, B., Hambly, N.C., & Adams, J.D. 2001a, *ApJSS*, 134, 103
- Barrado y Navascués, D., Zapatero Osorio, M. R., Béjar, V. J. S., Rebolo, R., Martín, E. L., Mundt, R., Bailer-Jones, C. A. L. 2001b, *A & A*, 377, L9
- Barrado y Navascués, D., Stauffer, J.R., Bouvier, J., & Martín, E.L. 2001c, *ApJ*, 555, 546
- Béjar, V.J.S., Zapatero Osorio, M.R., & Rebolo, R. 1999, *ApJ*, 521, 671
- Béjar, V.J.S., Martín, E. L., Zapatero Osorio, M. R., Rebolo, R., et al. 2001, *ApJ*, 556, 830
- Berriman, G., & Reid, N. 1987, *MNRAS*, 227, 315
- Bessell, M. S., & Brett, J. M. 1988, *PASP*, 100, 1134
- Boss, A. 2001, *ApJ*, 551, L432
- Bouvier, J., Stauffer, J.R., Martín, E.L., Barrado y Navascués, D., Wallace, B., & Béjar, V.J.S. 1998, *A & A*, 336, 490
- Burrows, A., Marley, M., Hubbard, W.B., Lunine, J.I., Guillot, T., & Saumon, D. 1997, *ApJ*, 491, 856
- Chabrier, G. 2001, *ApJ*, 554, 1274
- Chabrier, G., Baraffe, I., Allard, F., & Hauschildt, P. 2000, *ApJ*, 542, 464
- Cosburn, M.R., Hodgkin, S.T., Jameson, R.F., & Pinfield, D.J. 1997, *MNRAS*, 288, L23
- Crawford, D.L., & Perry, C.L. 1976, *AJ*, 81, 419
- D'Antona, F., & Mazzitelli, I. 1997, *Mem. Soc. Astron. Italiana*, 68, 4

- Festin, L. 1998, *A & A*, 333, 497
- Fukugita, M., Hogan, C. J., & Peebles, P. J. E. 1998, *ApJ*, 503, 518
- Gizis, J.E., Reid, I.N., & Monet, D.G. 1999, *AJ*, 118, 997
- Hambly, N.C., Hodgkin, S.T., Cossburn, M.R., & Jameson, R.F. 1999, *MNRAS*, 303, 835
- Hambly, N.C., Steele, I.A., Hawkins, M.R.S., & Jameson, R.F. 1995, *MNRAS*, 273, 505
- Herbig, G.H. 1998, *ApJ*, 497, 736
- Hillenbrand, L.A., & Hartman, L.W. 1997, *ApJ*, 492, 540
- Jameson, R.F., & Skillen, W.J.I., 1989, *MNRAS*, 239, 247
- Koorneef, J. 1983, *A & A*, 128, 84
- Kroupa, P. 1995, *MNRAS*, 277, 1522
- Kroupa, P., Tout, C.A., & Gilmore, G. 1993, *MNRAS*, 262, 545
- Lada, C.J., & Lada, E.A. 1991, The formation and evolution of star clusters, *ASP Conf. Ser* 13, p3
- Lada, E.A., & Lada, C.J. 1995, *AJ*, 109, 1682
- Larson, R.B. 1992, *MNRAS*, 256, 641
- Lee, T.A. 1968, *ApJ*, 152, 913
- Leggett, S.K. 1992, *ApJS*, 82, 351
- Lucas, P.W., & Roche, P.F. 2000, *MNRAS*, 314, 858
- Luhman, K.L., Rieke, G.H., Lada, C.J., & Lada, E.A. 1998, *ApJ*, 508, 347
- Luhman, K.L. 1999, *ApJ*, 525, 466
- Luhman, K.L., Liebert, J., & Rieke, G.H. 1999, *ApJ*, 489, L165
- Lynga, G. 1983, 5th Ceskoslovenska Akademie Conf., Star Clusters and Associations and Their Relation to the Evolution of the Galaxy, p80
- Magazzù, A., Rebolo, R., Zapatero Osorio, M.R., Martín, E.L., & Hodgkin, S.T. 1998, *ApJ*, 497, L47
- Martín et al. 2000, *ApJ*, 543, 299
- Miller, G.E., & Scalo, J.M. 1979, *ApJS*, 41, 513
- Muench, A.A., Alves, J., Lada, C.J., & Lada, E.A. 2001, *ApJ*, 558, L51
- Najita, J.R., Tiede, G.P., & Carr, J.S. 2000, *ApJ*, 541, 977
- Pinfield, D.J., Hodgkin, S.T., Jameson, R.F., Cossburn, M.R., & von Hippel, T. 1997, *MNRAS*, 287, 180
- Price, N.M., & Podsiadlowski, Ph. 1995, *MNRAS*, 273, 1041

- Raboud, D., & Mermilliod, J.-C. 1998, *A & A*, 333, 897
- Rebolo, R., Zapatero Osorio, M.R., & Martín, E.L. 1995, *Nature*, 377, 129
- Reid, I.N., & Hawley, L.S. 1999, *AJ*, 117, 343
- Reid, I.N., Kirkpatrick, J.D., et al. 1999, *ApJ*, 521, 613
- Reipurth, B., & Clarke, C. 2001, *ApJ*, 122, 432
- Rieke, G.H., & Lebofsky, M.J. 1985, *ApJ*, 288, 618
- Salpeter, E.E. 1955, *ApJ*, 121, 161
- Scalo, J.M. 1986, *Fundam. Cosmic Phys.*, 11, 1
- Simons, D.A., & Becklin, E.E. 1992, *ApJ*, 390, 431
- Spitzer, L.Jr., & Mathieu, R.D. 1980, *ApJ*, 241, 618
- Stauffer, J.R., Hamilton, D., Probst, R.G., Rieke, G., Mateo, M. 1989, *ApJ*, 344, L21
- Stauffer, J.R., Hamilton, D., Probst, R.G. 1994, *AJ*, 108, 155
- Stauffer, J.R., Barrado y Navascués, D., et al. 1999, *AJ*, 527, 219
- Walter, F.M., Vrba, F.J., Mathieu, R.D., Brown, A., & Myers, P.C. 1994, *AJ*, 107, 692
- White, R.J., Ghez, A.M., Reid, I.N., & Schultz, G. 1999, *ApJ*, 520, 811
- Wilking, B.A., Greene, T.P., & Meyer, M.R. 1999, *AJ*, 117, 469
- Wolk, S.J. 1996, Ph.D. thesis, Univ. New York at Stony Brook
- Zapatero Osorio, M.R., Béjar, V.J.S., Rebolo, R., Martín, E.L., & Basri, G. 1999a, *ApJ*, 524, L115
- Zapatero Osorio, M.R., Rebolo, R., Martín, E.L., Hodgkin, S.T., Cossburn, M.R., Magazzù, A., Steele, I.A., & Jameson, R.F. 1999b, *A & AS*, 134, 537
- Zapatero Osorio, M.R., Martín, E.L., & Rebolo, R. 1997, *A & A*, 323, 105
- Zapatero Osorio, M.R., Rebolo, R., Martín, E.L., & García López, R.J. 1996, *A & A*, 305, 519
- Zapatero Osorio, M.R., Béjar, V.J.S., Martín, E.L., Rebolo, R., Barrado y Navascués, D., Bailer-Jones, C.A.L., & Mundt, R. 2000, *Science*, 290, 103

Table 1: Mass limits for the three clusters

Passband	Limiting Mag.	Corresponding Mass(M_{\odot})		
		IC 348	σ Orionis	Pleiades
<i>J</i>	16.5	0.025	0.025	0.04
<i>H</i>	15.5	0.025	0.025	0.04
<i>K</i>	15.0	0.025	0.025	0.04
<i>F</i>	21.0	0.025	0.025	0.04

Table 2: Positions of the Field Centers

Fields	R.A. (J2000.0) (hh mm ss)	Decl. (J2000.0) (dd mm ss)	Radius (arcmin)
IC 348	03 44 30	+32 17 00	20
Control 1	03 49 08	+31 19 08	20
Control 2	03 44 10	+33 19 26	20
σ Orionis	05 38 45	-02 36 00	30
Control 1	05 58 29	-04 29 48	30
Control 2	05 11 00	-00 20 00	30
Pleiades	03 47 00	+24 07 00	90
Control 1	03 18 00	+26 41 00	90
Control 2	03 05 00	+24 42 00	90

Table 3: Summary of Results

Cluster	Age (Myr)	Distance (pc)	Mass Range (M_{\odot})	α
IC 348	5	316	0.5 – 0.035	0.7
σ Orionis	3	352	0.5 – 0.045	1.1
Pleiades	100	125	0.5 – 0.055	0.5